American Mineralogist, Volume 92, pages 309–327, 2007

Elastic anomalies accompanying phase transitions in (Ca,Sr)TiO_3 perovskites: Part I. Landau theory and a calibration for $SrTiO_3$

MICHAEL A. CARPENTER*

Department of Earth Sciences, University of Cambridge, Downing Street, Cambridge CB2 3EQ, U.K.

ABSTRACT

Landau theory has been used to develop expressions for the elastic anomalies that accompany octahedral tilting transitions in perovskites that are associated with the M and R points of the Brillouin zone. The master equation is a 246 Landau potential with saturation terms that provides phenomenological descriptions of transition sequences from a parent cubic structure through tetragonal or rhombohedral intermediates to orthorhombic or monoclinic product structures. Data from the literature have been used to determine values for all the coefficients required to generate a quantitative description of the $Pm\bar{3}m \leftrightarrow I4/mcm$ transition in $SrTiO_3$, which is taken as a model system. Solutions to the Landau expansion have been adapted to include the general influence of hydrostatic pressure and non-hydrostatic stress on transition temperature and the evolution of the order parameter. Critical examination of elastic constant data from the literature reveals inconsistencies between the results of measurements on tetragonal samples using ultrasonic rather than Brillouin scattering methods. An internally consistent data set has, nevertheless, been assembled. Good qualitative agreement was obtained between the general pattern of calculated and observed variations of all the single crystal elastic constants, and semi-quantitative agreement was obtained for C_{11}, C_{33}, C_{12}, and C_{13}. Some inconsistencies remain in relation to the temperature dependence of the square of the soft mode frequencies in the tetragonal phase, which follow the square of the order parameter rather than its inverse susceptibility, but the 246 potential seems to provide a good description of the structural evolution of $SrTiO_3$ over a wide temperature interval up to the cubic-tetragonal transition point.

Keywords: Phase transitions, Landau theory, perovskite, $SrTiO_3$

INTRODUCTION

There has been some debate in the literature as to whether the structure of silicate perovskites is cubic, tetragonal, or orthorhombic at the pressure-temperature conditions of the Earth's mantle. Current consensus appears to be that the orthorhombic (*Pnma*) structure is most likely to be the stable form of (Mg,Fe)SiO_3 (Wentzcovitch et al. 1993; Stixrude and Cohen 1993; Fiquet et al. 1998; Ono et al. 2004a; and references therein). For $CaSiO_3$, the most recent experimental and computational results appear to be favoring a view that the cubic ($Pm\bar{3}m$) structure may be stable at mantle conditions and that the tetragonal ($I4/mcm$) structure is the stable state at ambient conditions (Ono et al. 2004b; Kurashina et al. 2004; Caracas et al. 2005; Jung and Oganov 2005). Addition of Al stabilizes the orthorhombic structure (Kurashina et al. 2004). It is well known that substantial anomalies in the elastic properties of perovskites occur if they undergo structural phase transitions, and the influence of an individual transition might extend to pressures and temperatures which are well away from the transition point itself (e.g., Carpenter and Salje 1998). Since our understanding of the mantle depends in large part on seismic velocity data which, in turn, depend on the bulk modulus and shear modulus of each of the constituent minerals, considerable efforts have been expended in trying to produce quantitative data for the elastic properties of silicate perovskites. Working directly on the silicate perovskites themselves has been problematic because of the necessity of maintaining high confining pressures to prevent breakdown to other mineral assemblages. Bulk moduli can be obtained from static X-ray diffraction experiments (e.g., Ono et al. 2004a, and references therein), but measuring the shear modulus in-situ at high P and T is much more difficult. The tendency has therefore been to turn to analog systems, which are expected to show similar properties and patterns of structural evolution but have phase transitions in P-T ranges that are more amenable to investigation using currently available in-situ methods. One such analog system is the $CaTiO_3$-$SrTiO_3$ solid solution. It contains cubic ($Pm\bar{3}m$), tetragonal ($I4/mcm$), and orthorhombic (*Pnma*) forms, with structures that are believed to be exactly analogous to those of the silicate perovskites. Phase transitions between these forms can be induced by changing composition, temperature, or pressure under laboratory conditions (e.g., Mitsui and Westphal 1961; Guyot et al. 1993; Bianchi et al. 1994; Redfern 1996; Grzechnik et al. 1997; Ball et al. 1998; Kennedy et al. 1999; Qin et al. 2000, 2002; Carpenter et al. 2001; Ranjan et al. 2001; Ranjan and Pandey 2001a, 2001b; Yamanaka et al. 2002; Harrison et al. 2003; Ranson et al. 2005; Mishra et al. 2005, 2006a, 2006b). Thus the issue of elasticity as a function of structure type and as a function of transition mechanism can be addressed, with the expectation that the phenomenology will be the same for

* E-mail: mc43@esc.cam.ac.uk

perovskites in the mantle even if the details are different.

The purpose of the present set of three papers, of which this is the first, is to develop a quantitative model for the elastic constant variations that accompany phase transitions in $(Ca,Sr)TiO_3$ perovskites when composition, temperature, and pressure are varied. The starting point is an analysis of the $Pm\bar{3}m \leftrightarrow I4/mcm$ transition. The formal framework of Landau theory is first set out to describe octahedral tilting transitions in perovskites, in general. Values for all the coefficients required to describe the cubic ↔ tetragonal transition in $SrTiO_3$ are then determined using data from the literature. The results provide the basis for a quantitative model of how the single crystal elastic constants, bulk modulus, and shear modulus evolve through the transition point. In the second paper (Carpenter 2007), the model is developed further to describe the effects of pressure and changing composition across the $CaTiO_3$-$SrTiO_3$ solid solution. The elastic properties of tetragonal $(Ca,Sr)TiO_3$ crystals are highly sensitive also to the mobility of transformation twin walls (Schranz et al. 1999; Kityk et al. 2000a, 2000b; Binder and Knorr 2001; Lemanov et al. 2002; Harrison et al. 2003). This superelastic behavior is therefore reanalyzed in the light of the quantitative results for the intrinsic effects of the symmetry change alone. In the third paper (Carpenter et al. 2007), the overall Landau approach is tested against data for the bulk and shear moduli determined at room temperature as a function of composition across the $(Ca,Sr)TiO_3$ solid solution and as a function of pressure for two samples with different (Sr-rich) compositions.

The literature on phase transitions in $SrTiO_3$ is vast. Indeed, the $Pm\bar{3}m \leftrightarrow I4/mcm$ transition is widely regarded as providing the archetypical model for relationships between soft modes, symmetry breaking mechanisms, and changes in physical properties at structural phase transitions. Contrasting views of the transition have been summarized by Cowley (1996) and Salje et al. (1998). Cowley (1996) explained deviations from the predictions of classical second order behavior (critical exponent, $\beta = 1/2$) as being due to critical fluctuations in a significant temperature interval below T_c ($\beta = 1/3$). A widespread acceptance that the transition is close to being classically second order in character, at least for temperatures away from T_c, has resulted in the use (until recently, Kityk et al. 2000a) of a standard Landau 24 potential for describing the elastic anomalies which accompany the transition (Laubereau and Zurek 1970; Slonczewski and Thomas 1970; Rehwald 1970a, 1970b; Lüthi and Moran 1970; Fossheim and Berre 1972; Okai and Yoshimoto 1975). Salje et al. (1998) and Hayward and Salje (1999) demonstrated, however, that the deviation from $\beta = 1/2$ as $T \rightarrow T_c$ might be understood as being due to the proximity of a tricritical point ($\beta = 1/4$). They showed that a Landau 246 potential, which also includes terms to account for order parameter saturation as $T \rightarrow 0$ K, leads to a variation of the order parameter that is consistent with experimental data for excess heat capacity, spontaneous strain, birefringence, and octahedral tilt angles, from 0 K to within experimental uncertainty of the transition point (106 K). A necessary but not sufficient condition for the validity of any model of a phase transition is that it should reproduce the variations both of properties which depend on the first derivative of free energy, i.e., those which scale with equilibrium values of the order parameter, and of properties which depend on the second derivative of free energy, i.e., those which depend on susceptibility. The latter include elastic constants and the frequencies of soft modes. As well as providing a template for describing all octahedral tilt transitions associated with the M and R points of the Brillouin zone, therefore, the analysis of elastic anomalies in $SrTiO_3$ given here represents a test of the 246 potential proposed by Salje et al. (1998).

LANDAU THEORY

Master equation

A Landau expansion for $Pm\bar{3}m$ structures transforming to structures with symmetry subgroups associated with the M_3^+ and R_4^+ special points of the Brillouin zone is (after Carpenter et al. 2001):

$$
\begin{aligned}
G = {} & \frac{1}{2}a_1\Theta_{s1}\left(\coth\left(\frac{\Theta_{s1}}{T}\right)-\coth\left(\frac{\Theta_{s1}}{T_{c1}}\right)\right)\left(q_1^2+q_2^2+q_3^2\right) \\
& +\frac{1}{2}a_2\Theta_{s2}\left(\coth\left(\frac{\Theta_{s2}}{T}\right)-\coth\left(\frac{\Theta_{s2}}{T_{c2}}\right)\right)\left(q_4^2+q_5^2+q_6^2\right) \\
& +\frac{1}{4}b_1\left(q_1^2+q_2^2+q_3^2\right)^2+\frac{1}{4}b_1'\left(q_1^4+q_2^4+q_3^4\right) \\
& +\frac{1}{4}b_2\left(q_4^2+q_5^2+q_6^2\right)^2+\frac{1}{4}b_2'\left(q_4^4+q_5^4+q_6^4\right) \\
& +\frac{1}{6}c_1\left(q_1^2+q_2^2+q_3^2\right)^3+\frac{1}{6}c_1'\left(q_1q_2q_3\right)^2 \\
& +\frac{1}{6}c_1''\left(q_1^2+q_2^2+q_3^2\right)\left(q_1^4+q_2^4+q_3^4\right)+\frac{1}{6}c_2\left(q_4^2+q_5^2+q_6^2\right)^3 \\
& +\frac{1}{6}c_2'\left(q_4q_5q_6\right)^2+\frac{1}{6}c_2''\left(q_4^2+q_5^2+q_6^2\right)\left(q_4^4+q_5^4+q_6^4\right) \\
& +\lambda_q\left(q_1^2+q_2^2+q_3^2\right)\left(q_4^2+q_5^2+q_6^2\right) \\
& +\lambda_q'\left(q_1^2q_4^2+q_2^2q_5^2+q_3^2q_6^2\right)+\lambda_1e_a\left(q_1^2+q_2^2+q_3^2\right) \\
& +\lambda_2e_a\left(q_4^2+q_5^2+q_6^2\right)+\lambda_3\left[\sqrt{3}e_o\left(q_2^2-q_3^2\right)+e_t\left(2q_1^2-q_2^2-q_3^2\right)\right] \\
& +\lambda_4\left[\sqrt{3}e_o\left(q_5^2-q_6^2\right)+e_t\left(2q_4^2-q_5^2-q_6^2\right)\right] \\
& +\lambda_5\left(e_4q_4q_6+e_5q_4q_5+e_6q_5q_6\right)+\lambda_6\left(q_1^2+q_2^2+q_3^2\right)\left(e_4^2+e_5^2+e_6^2\right) \\
& +\lambda_7\left(q_1^2e_6^2+q_2^2e_4^2+q_3^2e_5^2\right)+\frac{1}{4}\left(C_{11}^o-C_{12}^o\right)\left(e_o^2+e_t^2\right) \\
& +\frac{1}{6}\left(C_{11}^o+2C_{12}^o\right)e_a^2+\frac{1}{2}C_{44}^o\left(e_4^2+e_5^2+e_6^2\right).
\end{aligned}
\tag{1}
$$

Here, q_1–q_6 are the order parameter components; a_1, a_2, b_1, etc., are normal Landau coefficients; Θ_{s1}, Θ_{s2} are saturation temperatures; T_{c1}, T_{c2} are critical temperatures; λ_1, λ_q, etc., are coupling coefficients; C_{11}^o, C_{12}^o, C_{44}^o are bare elastic constants; and e_4, e_5, e_6 are shear strain components. The symmetry-adapted strains e_a, e_o, and e_t are combinations of the linear strain components e_1, e_2, and e_3 as

$$e_a = (e_1 + e_2 + e_3) \tag{2}$$

$$e_o = (e_1 - e_2) \tag{3}$$

$$e_t = \frac{1}{\sqrt{3}}\left(2e_3 - e_1 - e_2\right). \tag{4}$$

Only the lowest order strain-order parameter coupling terms have been included. Direct biquadratic coupling, $\lambda_q q_1^2 q_4^2$, etc., is included for completeness although the coupling mechanism

might be indirectly via the common strain, in which case the direct coupling terms would not be required. This master equation is the same as given by Carpenter et al. (2001), except that saturation temperatures are now included to account for the way that the order parameter levels off as $T \rightarrow 0$ K (Salje et al. 1991a, 1991b). Table 1 lists the different possible space groups for product structures described by this free energy expansion. Relationships between their order parameter components are also given. The orientations of crystallographic axes with respect to the reference system, X, Y, Z of Equation 1 are reproduced in Figure 1 for *I*4/*mcm, Pnma*, and *P*4/*mbm* structures (after Carpenter et al. 2001).

R point

Transitions from $Pm\bar{3}m$ to *I*4/*mcm, Imma* or $R\bar{3}c$ structures involve only the order parameter components q_4, q_5, and q_6, and are expected to occur according to the 246 potential:

$$G = \frac{1}{2}a_2\Theta_{s2}\left(\coth\left(\frac{\Theta_{s2}}{T}\right) - \coth\left(\frac{\Theta_{s2}}{T_{c2}}\right)\right)\left(q_4^2+q_5^2+q_6^2\right) + \frac{1}{4}b_2\left(q_4^2+q_5^2+q_6^2\right)^2 + \frac{1}{4}b_2'\left(q_4^4+q_5^4+q_6^4\right) + \frac{1}{6}c_2\left(q_4^2+q_5^2+q_6^2\right)^3 + \frac{1}{6}c_2'\left(q_4q_5q_6\right)^2 + \frac{1}{6}c_2''\left(q_4^2+q_5^2+q_6^2\right)\left(q_4^4+q_5^4+q_6^4\right) + \lambda_2 e_a\left(q_4^2+q_5^2+q_6^2\right) + \lambda_4\left[\sqrt{3}e_o\left(q_5^2-q_6^2\right) + e_t\left(2q_4^2-q_5^2-q_6^2\right)\right] + \lambda_5\left(e_4q_4q_6 + e_5q_4q_5 + e_6q_5q_6\right) + \frac{1}{4}\left(C_{11}^o - C_{12}^o\right)\left(e_o^2+e_t^2\right) + \frac{1}{6}\left(C_{11}^o + 2C_{12}^o\right)e_a^2 + \frac{1}{2}C_{44}^o\left(e_4^2+e_5^2+e_6^2\right). \quad (5)$$

Relationships between strains and order parameter components are given by the equilibrium condition, $\partial G/\partial e = 0$, yielding

$$e_a = -\frac{\lambda_2\left(q_4^2+q_5^2+q_6^2\right)}{\frac{1}{3}\left(C_{11}^o+2C_{12}^o\right)} \quad (6)$$

$$e_o = -\frac{\lambda_4\sqrt{3}\left(q_5^2-q_6^2\right)}{\frac{1}{2}\left(C_{11}^o-C_{12}^o\right)} \quad (7)$$

$$e_t = -\frac{\lambda_4\left(2q_4^2-q_5^2-q_6^2\right)}{\frac{1}{2}\left(C_{11}^o-C_{12}^o\right)} \quad (8)$$

$$e_4 = -\frac{\lambda_5 q_4 q_6}{C_{44}^o} \quad (9)$$

$$e_5 = -\frac{\lambda_5 q_4 q_5}{C_{44}^o} \quad (10)$$

TABLE 1. Order parameter components for the symmetry subgroups of $Pm\bar{3}m$ associated with special points M_3^+ and R_4^+ (after Howard and Stokes 1998; Carpenter et al. 2001)

Space group	Order parameter components M_3^+	R_4^+	Relationships between order parameter components
$Pm\bar{3}m$	000	000	
*P*4/*mbm*	$q_1$00	000	
*I*4/*mmm*	$q_1 0 q_3$	000	$q_1 = q_3$
Im$\bar{3}$	$q_1 q_2 q_3$	000	$q_1 = q_2 = q_3$
Immm	$q_1 q_2 q_3$	000	$q_1 \neq q_2 \neq q_3$
*I*4/*mcm*	000	$q_4$00	
Imma	000	$q_4 0 q_6$	$q_4 = q_6$
*R*3*c*	000	$q_4 q_5 q_6$	$q_4 = q_5 = q_6$
*C*2/*m*	000	$q_4 0 q_6$	$q_4 \neq q_6$
*C*2/*c*	000	$q_4 q_5 q_6$	$q_4 = q_6 \neq q_5$
P$\bar{1}$	000	$q_4 q_5 q_6$	$q_4 \neq q_5 \neq q_6$
Cmcm	$00 q_3$	$q_4$00	$q_3 \neq q_4$
Pnma	$0 q_2 0$	$q_4 0 q_6$	$q_2 \neq q_4 = q_6$
$P2_1/m$	$0 q_2 0$	$q_4 0 q_6$	$q_2 \neq q_4 \neq q_6$
$P4_2/nmc$	$0 q_2 q_3$	$q_4$00	$q_2 = q_3 \neq q_4$

Note: The system of reference axes for these components is that used in Stokes and Hatch (1988) and the group theory program ISOTROPY.

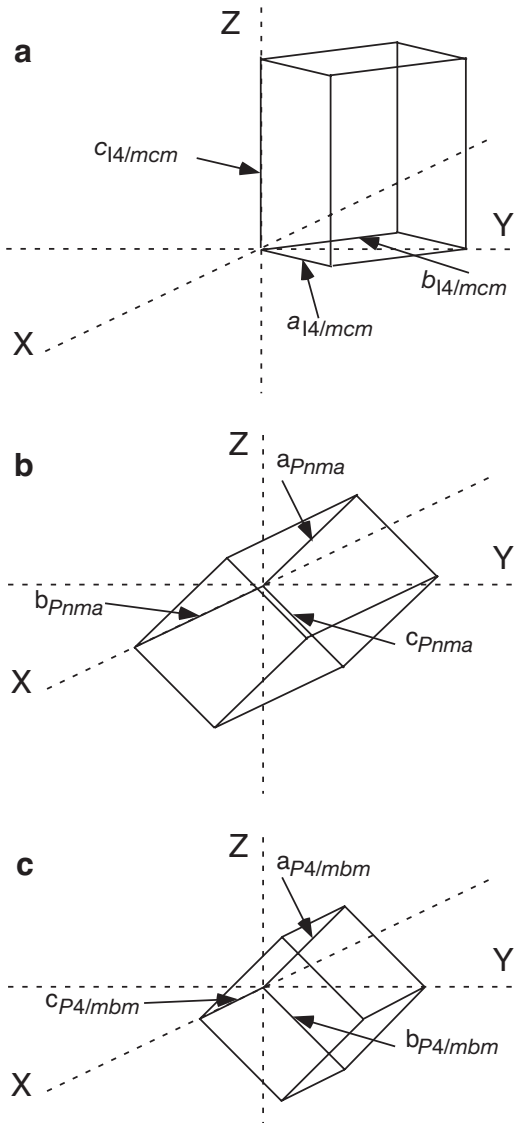

FIGURE 1. Relationships between unit-cell orientations and reference axes for the order parameter/strain coupling terms in Equation 1. (**a**) *I*4/*mcm*, $q_4 \neq 0$, $q_5 = q_6 = 0$. The same orientation applies to *P*4/*mbm* with $q_1 \neq 0$, $q_2 = q_3 = 0$, though the c parameter of the *I*4/*mcm* structure is double that of the *P*4/*mbm* structure. (**b**) Orientation relationship for $q_5 = 0$, $q_4 = q_6 \neq 0$ in both *Imma* and *Pnma* structures. (**c**) Orientation of crystallographic axes for the *P*4/*mbm* structure with $q_2 \neq 0$, $q_1 = q_3 = 0$.

$$e_6 = -\frac{\lambda_5 q_5 q_6}{C_{44}^o}. \quad (11)$$

Substituting these relationships back into Equation 5 gives the renormalized form of the Landau expansion as

$$\begin{aligned} G = {} & \frac{1}{2}a_2\Theta_{s2}\left(\coth\left(\frac{\Theta_{s2}}{T}\right) - \coth\left(\frac{\Theta_{s2}}{T_{c2}}\right)\right)\left(q_4^2 + q_5^2 + q_6^2\right) \\ & + \frac{1}{4}b_2^*\left(q_4^2 + q_5^2 + q_6^2\right)^2 + \frac{1}{4}b_2^{'*}\left(q_4^4 + q_5^4 + q_6^4\right) \\ & + \frac{1}{6}c_2\left(q_4^2 + q_5^2 + q_6^2\right)^3 + \frac{1}{6}c_2'\left(q_4 q_5 q_6\right)^2 \\ & + \frac{1}{6}c_2''\left(q_4^2 + q_5^2 + q_6^2\right)\left(q_4^4 + q_5^4 + q_6^4\right), \end{aligned} \quad (12)$$

where

$$b_2^* = b_2 - \frac{\lambda_5^2}{C_{44}^o} - \frac{2\lambda_2^2}{\frac{1}{3}\left(C_{11}^o + 2C_{12}^o\right)} + \frac{4\lambda_4^2}{\frac{1}{2}\left(C_{11}^o - C_{12}^o\right)} \quad (13)$$

$$b_2^{'*} = b_2' + \frac{\lambda_5^2}{C_{44}^o} - \frac{12\lambda_4^2}{\frac{1}{2}\left(C_{11}^o - C_{12}^o\right)}. \quad (14)$$

Equation 12 is essentially the same as the general 246 potential considered by Vanderbilt and Cohen (2001), except that the effects of saturation are now accounted for, and the high order terms are grouped slightly differently. If the excess free energy is dominated by the second and fourth order terms such that the expansion can be truncated to exclude sixth order terms, only the tetragonal and rhombohedral structures can be stable. Thomas and Müller (1968) showed that the orthorhombic phase will always be intermediate in energy between these two (see, also, Harley et al. 1973; Birgeneau et al. 1974; Darlington 1997). The stability criteria of Thomas and Müller, adapted to the slightly different combination of fourth order terms used here, are: $b_2^{'*} < 0$ gives *I*4/*mcm* as the stable form and $b_2^{'*} > 0$ gives $R\bar{3}c$ as the stable form.

The influence of sixth order terms is such that each of the tetragonal, orthorhombic, and rhombohedral structures can be stable, depending on the actual values of the coefficients (Devonshire 1949; Vanderbilt and Cohen 2001). Expressing Devonshire's stability criteria in terms of the renormalized fourth order coefficients used here, $R\bar{3}c$ or *I*4/*mcm* structures will be stable for $(b_2^* + b_2^{'*}) > 0$, $b_2^* > 0$, but a sequence of stability cubic ↔ tetragonal ↔ orthorhombic ↔ rhombohedral can develop with falling temperature if the values of the fourth order coefficients are such that $(b_2^* + b_2^{'*}) < 0$, $b_2^* > 0$.

For the case of $SrTiO_3$, Hayward and Salje (1999) have shown that a 246 potential with a positive value of $(b_2^* + b_2^{'*})$ can be used to describe the order parameter evolution and excess entropy due to the $Pm\bar{3}m \leftrightarrow$ *I*4/*mcm* transition at 106 K. Their solution for q_4 ($q_5 = q_6 = 0$), with all the relevant fourth order and sixth order coefficients shown explicitly, is

$$q_4^2 = \frac{-\left(b_2^* + b_2^{'*}\right) + \sqrt{\left(b_2^* + b_2^{'*}\right)^2 + 4a_2\left(c_2 + c_2''\right)\Theta_{s2}\left(\coth\left(\frac{\Theta_{s2}}{T_{c2}}\right) - \coth\left(\frac{\Theta_{s2}}{T}\right)\right)}}{2\left(c_2 + c_2''\right)}. \quad (15)$$

Solutions for the order parameter as a function of temperature for metastable *Imma* and $R\bar{3}c$ structures are, respectively:

$$2q_4^2 = \frac{-\left(b_2^* + \frac{1}{2}b_2^{'*}\right) + \sqrt{\left(b_2^* + \frac{1}{2}b_2^{'*}\right)^2 + 4a_2\left(c_2 + \frac{1}{2}c_2''\right)\Theta_{s2}\left(\coth\left(\frac{\Theta_{s2}}{T_{c2}}\right) - \coth\left(\frac{\Theta_{s2}}{T}\right)\right)}}{2\left(c_2 + \frac{1}{2}c_2''\right)} \quad (16)$$

$$3q_4^2 = \frac{-\left(b_2^* + \frac{1}{3}b_2^{'*}\right) + \sqrt{\left(b_2^* + \frac{1}{3}b_2^{'*}\right)^2 + 4a_2\left(c_2 + \frac{1}{27}c_2' + \frac{1}{3}c_2''\right)\Theta_{s2}\left(\coth\left(\frac{\Theta_{s2}}{T_{c2}}\right) - \coth\left(\frac{\Theta_{s2}}{T}\right)\right)}}{2\left(c_2 + \frac{1}{27}c_2' + \frac{1}{3}c_2''\right)}. \quad (17)$$

Expressions for the individual elastic constants of the *I*4/*mcm* structure, maintaining the reference system of the cubic parent structure, are given in the usual way by applying

$$C_{ik} = C_{ik}^o - \sum_m \frac{\partial^2 G}{\partial e_i \partial q_m} \cdot \left(\frac{\partial^2 G}{\partial q_m^2}\right)^{-1} \cdot \frac{\partial^2 G}{\partial e_k \partial q_m}, \quad (18)$$

from Slonczewski and Thomas (1970), to Equation 5 (see, also, Bulou et al. 1992). Expressions for the individual elastic constants are listed in Table 2. They differ from those given in earlier studies of the elastic properties of $SrTiO_3$ (e.g., Slonczewski and Thomas 1970; Rehwald 1970b, 1971; Lüthi and Moran 1970; Fossheim and Berre 1972; Bulou et al. 1992; Ishidate et al. 1988) in that they include all the sixth order terms and terms to account for order parameter saturation. Kityk et al. (2000a) used a 246 potential but included only one sixth order coefficient. Equivalent expressions for the elastic constants accompanying a $Pm\bar{3}m \leftrightarrow$ *Imma* transition, derived from Equations 5 and 16, are listed in Table 3. Elastic constants for the conventional *I*4/*mcm*

TABLE 2. Elastic constant variations expected in the stability field of a structure with *I*4/*mcm* symmetry ($q_4 \neq 0$, $q_5 = q_6 = 0$), due to a transition from a parent cubic structure with $Pm\bar{3}m$ symmetry

$C_{11} = C_{12} = C_{11}^o - M^2\chi_4 q_4^2$	$C_{13} = C_{23} = C_{12}^o - MN\chi_4 q_4^2$
$C_{33} = C_{11}^o - N^2\chi_4 q_4^2$	$C_{44} = C_{55} = C_{44}^o - \lambda_5^2\chi_6 q_4^2$
$C_{12} = C_{12}^o - M^2\chi_4 q_4^2$	$C_{66} = C_{44}^o$

* $K_V = \frac{1}{3}\left(C_{11}^o + 2C_{12}^o\right) - 4\lambda_2^2\chi_4 q_4^2$

* $G_V = \frac{1}{5}\left(C_{11}^o - C_{12}^o + 3C_{44}^o\right) - \frac{2}{5}\left(8\lambda_4^2\chi_4 + \lambda_5^2\chi_6\right)q_4^2$

† $\chi_4^{-1} = \partial^2 G/\partial q_4^2 = 2(b_2 + b_2')q_4^2 + 4(c_2 + c_2'')q_4^4$

† $\chi_6^{-1} = \partial^2 G/\partial q_6^2 = \left[\frac{12\lambda_4^2}{\frac{1}{2}\left(C_{11}^o - C_{12}^o\right)} - b_2'\right]q_4^2 - \frac{2}{3}c_2'' q_4^4$

$M = \left(2\lambda_2 - \frac{4}{\sqrt{3}}\lambda_4\right)$ $\quad$ $N = \left(2\lambda_2 + \frac{8}{\sqrt{3}}\lambda_4\right)$

Elastic constants, $C_{ik,c}$, for a unit cell with conventional orientation (**a**//X, **b**//Y, **c**//Z)

$C_{11,c} = C_{22,c} = \frac{1}{2}\left(C_{11} + C_{12}\right) + C_{66}$	$C_{13,c} = C_{23,c} = C_{13}$
$C_{33,c} = C_{33}$	$C_{44,c} = C_{55,c} = C_{44}$
$C_{12,c} = \frac{1}{2}\left(C_{11} + C_{12}\right) - C_{66}$	$C_{66,c} = \frac{1}{2}\left(C_{11} - C_{12}\right)$

* Expressions for the Voigt limits of bulk and shear modulus in terms of single-crystal elastic constants for a crystal with point group 4/*mmm* were taken from Watt and Peselnik (1980).

† Values of q in the expressions for susceptibility are the equilibrium values given by Equation 15.

and *Imma* unit-cell orientations (**a**//X, **b**//Y, **c**//Z) are obtained by rotation of axes for a fourth rank tensor (Nye 1985), and are given in Tables 2 and 3 for completeness.

In the context of geophysical applications, bulk (K) and shear (G) moduli are required. These can be calculated from the individual elastic constants in the usual way using expressions for the Voigt (K_V, G_V) and Reuss (K_R, G_R) limits. Numerical values for these limits usually differ by less than a few percent. As the Voigt expressions show the influence of individual coupling parameters from the Landau expansion most clearly, they are listed in Tables 2 and 3 for each transition.

M point

Structures with *P*4/*mbm*, *I*4/*mmm*, or *Im*$\bar{3}$ symmetry have not been observed in the (Ca,Sr)TiO_3 system, but the *Pnma* structure has order parameter components associated with both the R and M points. In parallel with an analysis of the R point behavior, it is therefore necessary to explore behavior associated with the M point. Taking the same starting point as in the previous section, a cubic ↔ tetragonal or a cubic (P) ↔ cubic (I) transition would be expected to behave according to Equation 1 using terms in q_1, q_2 and q_3 alone:

$$\begin{aligned}G = {} & \frac{1}{2}a_1\Theta_{s1}\left(\coth\left(\frac{\Theta_{s1}}{T}\right)-\coth\left(\frac{\Theta_{s1}}{T_{c1}}\right)\right)\left(q_1^2+q_2^2+q_3^2\right)\\ & +\frac{1}{4}b_1\left(q_1^2+q_2^2+q_3^2\right)^2+\frac{1}{4}b_1'\left(q_1^4+q_2^4+q_3^4\right)\\ & +\frac{1}{6}c_1\left(q_1^2+q_2^2+q_3^2\right)^3+\frac{1}{6}c_1'\left(q_1q_2q_3\right)^2+\frac{1}{6}c_1''\left(q_1^2+q_2^2+q_3^2\right)\left(q_1^4+q_2^4+q_3^4\right)\\ & +\lambda_1 e_a\left(q_1^2+q_2^2+q_3^2\right)\\ & +\lambda_3\left[\sqrt{3}e_o\left(q_2^2-q_3^2\right)+e_t\left(2q_1^2-q_2^2-q_3^2\right)\right]\\ & +\lambda_6\left(q_1^2+q_2^2+q_3^2\right)\left(e_4^2+e_5^2+e_6^2\right)+\lambda_7\left(q_1^2e_6^2+q_2^2e_4^2+q_3^2e_5^2\right)\\ & +\frac{1}{4}\left(C_{11}^o-C_{12}^o\right)\left(e_o^2+e_t^2\right)+\frac{1}{6}\left(C_{11}^o+2C_{12}^o\right)e_a^2+\frac{1}{2}C_{44}^o\left(e_4^2+e_5^2+e_6^2\right).\end{aligned} \tag{19}$$

Applying the equilibrium condition for strain gives

$$e_a=\frac{-\lambda_1\left(q_1^2+q_2^2+q_3^2\right)}{\frac{1}{3}\left(C_{11}^o+2C_{12}^o\right)} \tag{20}$$

$$e_o=\frac{-\lambda_3\sqrt{3}\left(q_2^2-q_3^2\right)}{\frac{1}{2}\left(C_{11}^o-C_{12}^o\right)} \tag{21}$$

$$e_t=\frac{\lambda_3\left(2q_1^2-q_2^2-q_3^2\right)}{\frac{1}{2}\left(C_{11}^o-C_{12}^o\right)} \tag{22}$$

$$e_4=e_5=e_6=0. \tag{23}$$

Substituting these expressions back into Equation 19 gives

$$\begin{aligned}G = {} & \frac{1}{2}a_1\Theta_{s1}\left(\coth\left(\frac{\Theta_{s1}}{T}\right)-\coth\left(\frac{\Theta_{s1}}{T_{c1}}\right)\right)\left(q_1^2+q_2^2+q_3^2\right)\\ & +\frac{1}{4}b_1^*\left(q_1^2+q_2^2+q_3^2\right)^2+\frac{1}{4}b_1'^*\left(q_1^4+q_2^4+q_3^4\right)\\ & +\frac{1}{6}c_1\left(q_1^2+q_2^2+q_3^2\right)^3+\frac{1}{6}c_1'\left(q_1q_2q_3\right)^2+\frac{1}{6}c_1''\left(q_1^2+q_2^2+q_3^2\right)\left(q_1^4+q_2^4+q_3^4\right)\end{aligned} \tag{24}$$

TABLE 3. Elastic constant variations expected in the stability field of a structure with *Imma* symmetry ($q_4 = q_6 \neq 0$, $q_5 = 0$), due to a transition from a parent cubic structure with *Pm*$\bar{3}$*m* symmetry

$C_{11} = C_{11}^o - 2M^2\chi_4 q_4^2$	$C_{14} = -2M\lambda_5\chi_4 q_4^2$
$C_{22} = C_{11}^o - (M^2 + N^2)\chi_4 q_4^2$	$C_{24} = C_{34} = -(M + N)\lambda_5\chi_4 q_4^2$
$C_{33} = C_{11}^o - (N^2 + M^2)\chi_4 q_4^2$	$C_{56} = -\lambda_5^2\chi_5 q_4^2$
$C_{12} = C_{12}^o - (M^2 + MN)\chi_4 q_4^2$	$C_{44} = C_{44}^o - 2\lambda_5^2\chi_4 q_4^2$
$C_{13} = C_{12}^o - (MN + M^2)\chi_4 q_4^2$	$C_{55} = C_{66} = C_{44}^o - \lambda_5^2\chi_5 q_4^2$
$C_{23} = C_{12}^o - 2MN\chi_4 q_4^2$	

* $K_V = \frac{1}{3}\left(C_{11}^o + 2C_{12}^o\right) - 8\lambda_2^2\chi_4 q_4^2$

* $G_V = \frac{1}{5}\left(C_{11}^o - C_{12}^o + 3C_{44}^o\right) - \frac{2}{5}\left(16\lambda_4^2\chi_4 + \lambda_5^2\chi_4 + \lambda_5^2\chi_5\right)q_4^2$

† $\chi_4^{-1}\left(=\chi_6^{-1}\right) = \partial^2 G/\partial q_4^2 = \left(2b_2 + 2b_2' + \frac{\lambda_5^2}{C_{44}^o}\right)q_4^2 + \left(10c_2 + \frac{19}{3}c_2''\right)q_4^4$

† $\chi_5^{-1} = \partial^2 G/\partial q_5^2 = \left[\frac{\lambda_5^2}{C_{44}^o} + \frac{12\lambda_4^2}{\frac{1}{2}\left(C_{11}^o - C_{12}^o\right)} - b_2'\right]q_4^2 + \left(2c_2 + \frac{1}{3}c_2' - \frac{1}{3}c_2''\right)q_4^4$

Elastic constants, $C_{ik,c}$, for a unit cell with conventional orientation (**a**//X, **b**//Y, **c**//Z)

$C_{11,c} = \frac{1}{2}\left(C_{22} + C_{23}\right) + 2C_{24} + C_{44}$	$C_{23,c} = C_{12} - C_{14}$
$C_{22,c} = C_{11}$	$C_{44,c} = \frac{1}{2}\left(C_{55} + C_{66}\right) - C_{56}$
$C_{33,c} = \frac{1}{2}\left(C_{22} + C_{23}\right) - 2C_{24} + C_{44}$	$C_{55,c} = \frac{1}{2}\left(C_{22} - C_{23}\right)$
$C_{12,c} = C_{12} + C_{14}$	$C_{66,c} = \frac{1}{2}\left(C_{55} + C_{66}\right) + C_{56}$
$C_{13,c} = \frac{1}{2}\left(C_{22} + C_{23}\right) - C_{44}$	

* Expressions for the Voigt limits of bulk and shear modulus in terms of single-crystal elastic constants for an orthorhombic crystal were taken from Watt (1979).

† Values of q in the expressions for susceptibility are the equilibrium values given by Equation 16.

where

$$b_1^* = b_1 - \frac{2\lambda_1^2}{\frac{1}{3}\left(C_{11}^o + 2C_{12}^o\right)} + \frac{4\lambda_3^2}{\frac{1}{2}\left(C_{11}^o - C_{12}^o\right)} \tag{25}$$

$$b_1'^* = b_1' - \frac{12\lambda_3^2}{\frac{1}{2}\left(C_{11}^o - C_{12}^o\right)}. \tag{26}$$

Once again, the form of Equation 24 is essentially the same as the 246 expansion used by Vanderbilt and Cohen (2001) to show that all three product structures (*P*4/*mbm*, *I*4/*mmm*, *Im*$\bar{3}$) could have equilibrium stability fields, depending on the actual values of the coefficients. In the present context, the structure of interest is *P*4/*mbm* with $q_2 \neq 0$, $q_1 = q_3 = 0$ as this is a component of the *Pnma* structure (see Fig. 1c). Assuming that the sum of fourth order terms is positive, the evolution of q_2^2 due to a *Pm*$\bar{3}$*m* ↔ *P*4/*mbm* transition would be expected to follow

$$q_2^2 = \frac{-\left(b_1^* + b_1'^*\right) + \sqrt{\left(b_1^* + b_1'^*\right)^2 + 4a_1\left(c_1 + c_1''\right)\Theta_{s1}\left(\coth\left(\frac{\Theta_{s1}}{T_{c1}}\right) - \coth\left(\frac{\Theta_{s1}}{T}\right)\right)}}{2\left(c_1 + c_1''\right)}. \tag{27}$$

TABLE 4. Elastic constant variations expected in the stability field of a structure with *P4/mbm* symmetry ($q_2 \neq 0$, $q_1 = q_3 = 0$), due to a transition from a parent cubic structure with $Pm\bar{3}m$ symmetry

$C_{11} = C^o_{11} - P^2\chi_2 q_2^2$	$C_{23} = C^o_{12} - O^2\chi_2 q_2^2$
$C_{22} = C_{33} = C^o_{11} - O^2\chi_2 q_2^2$	$C_{44} = C^o_{44} + 2(\lambda_6 + \lambda_7)q_2^2$
$C_{12} = C_{13} = C^o_{12} - OP\chi_2 q_2^2$	$C_{55} = C_{66} = C^o_{44} + 2\lambda_6 q_2^2$

* $K_V = \frac{1}{3}\left(C^o_{11} + 2C^o_{12}\right) - 4\lambda_1^2\chi_2 q_2^2$

* $G_V = \frac{1}{5}\left(C^o_{11} - C^o_{12} + 3C^o_{44}\right) - \frac{2}{5}\left(8\lambda_3^2\chi_2 + 3\lambda_6 + 2\lambda_7\right)q_2^2$

† $\chi_2^{-1} = \partial^2 G/\partial q_2^2 = 2(b_1 + b_1')q_2^2 + 4(c_1 + c_1'')q_2^4$

$O = \left(2\lambda_1 - \frac{4}{\sqrt{3}}\lambda_3\right)$ $\qquad$ $P = \left(2\lambda_1 + \frac{8}{\sqrt{3}}\lambda_3\right)$

Elastic constants, $C_{ik,c}$, for a unit cell with conventional orientation (**a**//X, **b**//Y, **c**//Z)

$C_{11,c} = C_{22,c} = \frac{1}{2}\left(C_{22} + C_{23}\right) + C_{44}$	$C_{13,c} = C_{23,c} = C_{12}$
$C_{33,c} = C_{11}$	$C_{44,c} = C_{55,c} = C_{55}$
$C_{12,c} = \frac{1}{2}\left(C_{22} + C_{23}\right) - C_{44}$	$C_{66,c} = \frac{1}{2}\left(C_{22} - C_{23}\right)$

* Expressions for the Voigt limits of bulk and shear modulus in terms of single-crystal elastic constants for a crystal with point group 4/*mmm* were taken from Watt and Peselnik (1980).
† Values of q in the expressions for susceptibility are the equilibrium values given by Equation 27.

Changes in the single-crystal elastic constants accompanying such a transition are listed in Table 4.

Combined M + R point transitions

Phase transitions leading from the $Pm\bar{3}m$ perovskite structure to structures that have both M point and R point octahedral tilts, such as the *Cmcm* or *Pnma* structures, are described by the full Landau expansion with six order parameter components (Eq. 1). Applying the usual equilibrium conditions with respect to strain leads to general relationships between the order parameter components and symmetry-adapted strains as

$$e_a = -\left[\frac{\lambda_1\left(q_1^2 + q_2^2 + q_3^2\right) + \lambda_2\left(q_4^2 + q_5^2 + q_6^2\right)}{\frac{1}{3}\left(C^o_{11} + 2C^o_{12}\right)}\right] \tag{28}$$

$$e_o = -\left[\frac{\lambda_3\sqrt{3}\left(q_2^2 - q_3^2\right) + \lambda_4\sqrt{3}\left(q_5^2 - q_6^2\right)}{\frac{1}{2}\left(C^o_{11} - C^o_{12}\right)}\right] \tag{29}$$

$$e_t = -\left[\frac{\lambda_3\left(2q_1^2 - q_2^2 - q_3^2\right) + \lambda_4\left(2q_4^2 - q_5^2 - q_6^2\right)}{\frac{1}{2}\left(C^o_{11} - C^o_{12}\right)}\right] \tag{30}$$

$$e_4 = -\frac{\lambda_5 q_4 q_6}{2\lambda_6\left(q_1^2 + q_2^2 + q_3^2\right) + 2\lambda_7 q_2^2 + C^o_{44}} \tag{31}$$

$$e_5 = -\frac{\lambda_5 q_4 q_5}{2\lambda_6\left(q_1^2 + q_2^2 + q_3^2\right) + 2\lambda_7 q_3^2 + C^o_{44}} \tag{32}$$

$$e_6 = -\frac{\lambda_5 q_5 q_6}{2\lambda_6\left(q_1^2 + q_2^2 + q_3^2\right) + 2\lambda_7 q_1^2 + C^o_{44}}. \tag{33}$$

Substituting for strain in Equation 1 using these expressions {and making the simplifying assumption $C^o_{44} >> [2\lambda_6(q_1^2 + q_2^2 + q_3^2) + 2\lambda_7 q_i^2]$, $i = 1, 2$ or 3} leads to the renormalized form of Equation 1:

$$\begin{aligned}
G = {} & \frac{1}{2}a_1\Theta_{s1}\left(\coth\left(\frac{\Theta_{s1}}{T}\right) - \coth\left(\frac{\Theta_{s1}}{T_{c1}}\right)\right)\left(q_1^2 + q_2^2 + q_3^2\right) \\
& + \frac{1}{2}a_2\Theta_{s2}\left(\coth\left(\frac{\Theta_{s2}}{T}\right) - \coth\left(\frac{\Theta_{s2}}{T_{c2}}\right)\right)\left(q_4^2 + q_5^2 + q_6^2\right) \\
& + \frac{1}{4}b_1^*\left(q_1^2 + q_2^2 + q_3^2\right)^2 + \frac{1}{4}b_1'^*\left(q_1^4 + q_2^4 + q_3^4\right) \\
& + \frac{1}{4}b_2^*\left(q_4^2 + q_5^2 + q_6^2\right)^2 + \frac{1}{4}b_2'^*\left(q_4^4 + q_5^4 + q_6^4\right) \\
& + \frac{1}{6}c_1\left(q_1^2 + q_2^2 + q_3^2\right)^3 + \frac{1}{6}c_1'\left(q_1 q_2 q_3\right)^2 \\
& + \frac{1}{6}c_1''\left(q_1^2 + q_2^2 + q_3^2\right)\left(q_1^4 + q_2^4 + q_3^4\right) + \frac{1}{6}c_2\left(q_4^2 + q_5^2 + q_6^2\right)^3 \\
& + \frac{1}{6}c_2'\left(q_4 q_5 q_6\right)^2 + \frac{1}{6}c_2''\left(q_4^2 + q_5^2 + q_6^2\right)\left(q_4^4 + q_5^4 + q_6^4\right) \\
& + \lambda_q^*\left(q_1^2 + q_2^2 + q_3^2\right)\left(q_4^2 + q_5^2 + q_6^2\right) + \lambda_q'^*\left(q_1^2 q_4^2 + q_2^2 q_5^2 + q_3^2 q_6^2\right) \\
& + \lambda_5^2\lambda_6\left(q_1^2 + q_2^2 + q_3^2\right)\left(q_4^2 q_6^2 + q_4^2 q_5^2 + q_5^2 q_6^2\right).
\end{aligned} \tag{34}$$

Here, renormalization of the coupling coefficients, λ_q, λ_q', occurs because M point and R point tilts both give rise to strains which overlap and give

$$\lambda_q^* = \lambda_q - \frac{\lambda_1\lambda_2}{\frac{1}{3}\left(C^o_{11} + 2C^o_{12}\right)} + \frac{2\lambda_3\lambda_4}{\frac{1}{2}\left(C^o_{11} - C^o_{12}\right)} \tag{35}$$

$$\lambda_q'^* = \lambda_q' - \frac{6\lambda_3\lambda_4}{\frac{1}{2}\left(C^o_{11} - C^o_{12}\right)}. \tag{36}$$

Which of the phases with both M and R point tilts is stable depends again on the actual values of the various coefficients. For (Ca,Sr)TiO_3 perovskites, the first transition with falling temperature is from the cubic parent structure to the *I*4/*mcm* structure, indicating $T_{c2} > T_{c1}$. If the coefficients for M point transitions are more or less the same as for the R point transitions, two sequences of thermodynamically continuous transitions are possible: $Pm\bar{3}m \rightarrow I4/mcm \rightarrow Cmcm$ or $Pm\bar{3}m \rightarrow Imma \rightarrow Pnma$. In each case, the first transition occurs at T_{c2} and the second at T_{c1}. This is illustrated schematically in Figure 2a for the situation where the *Imma* structure always has higher energy than the *I*4/*mcm* structure. The free energy change due to a $Pm\bar{3}m \rightarrow ... \rightarrow Cmcm$ sequence is given by the combined energies of separate $Pm\bar{3}m \rightarrow P4/mbm$ ($q_3 \neq 0$, $q_1 = q_2 = 0$) and $Pm\bar{3}m \rightarrow I4/mcm$ ($q_4 \neq 0$, $q_5 = q_6 = 0$) transitions, plus the coupling energy:

$$\left[\lambda_q - \frac{\lambda_1\lambda_2}{\frac{1}{3}\left(C^o_{11} + 2C^o_{12}\right)} + \frac{2\lambda_3\lambda_4}{\frac{1}{2}\left(C^o_{11} - C^o_{12}\right)}\right]q_3^2 q_4^2.$$

The free energy change due to a $Pm\bar{3}m \rightarrow ... \rightarrow Pnma$ sequence is, likewise, the sum of energy changes due to separate

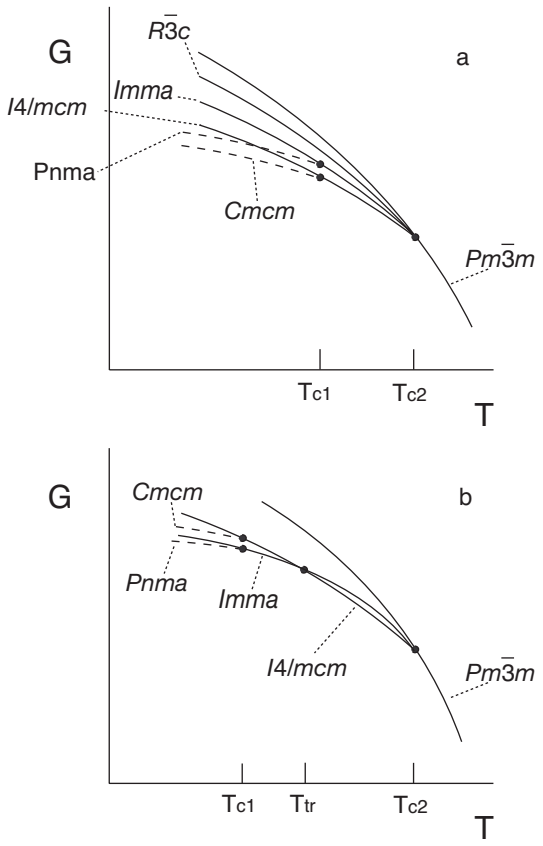

FIGURE 2. (**a**) Schematic free energy relationships between structures with no octahedral tilting ($T > T_{c2}$), M point octahedral tilting ($T_{c1} < T < T_{c2}$), and M+R point tilting ($T < T_{c1}$). These relationships represent circumstances in which the transitions at $T = T_{c2}$ are continuous and the *I*4/*mcm* structure is more stable than the *Imma* structure. (**b**) Schematic free energy relationships required for a sequence of equilibrium structural states $Pm\bar{3}m \rightarrow I4/mcm \rightarrow Imma \rightarrow Pnma$ with falling temperature.

$Pm\bar{3}m \rightarrow P4/mbm$ ($q_2 \neq 0$, $q_1 = q_3 = 0$) and $Pm\bar{3}m \rightarrow Imma$ ($q_4 = q_6 \neq 0$, $q_5 = 0$) transitions, plus a coupling energy:

$$\left[\lambda_q - \frac{\lambda_1\lambda_2}{\frac{1}{3}\left(C_{11}^o + 2C_{12}^o\right)} + \frac{2\lambda_3\lambda_4}{\frac{1}{2}\left(C_{11}^o - C_{12}^o\right)}\right]2q_2^2q_4^2 + \left[\frac{\lambda_5^2\left(\lambda_6 + \lambda_7\right)}{C_{44}^{o\,2}}\right]q_2^2q_4^4.$$

The coupling term in $q_2^2q_4^4$ is likely to be small in comparison with the term in $q_2^2q_4^2$, with the implication that, so long as the *I*4/*mcm* structure is stable with respect to the *Imma* structure, the *Cmcm* structure will be stable with respect to the *Pnma* structure. In this case, a first order transition $I4/mcm \rightarrow Pnma$ is possible, but only to a metastable state, and the equilibrium sequence will be $Pm\bar{3}m \rightarrow I4/mcm \rightarrow Cmcm$ (Fig. 2a).

To get an equilibrium stability field for the *Pnma* structure, it appears to be necessary for the *Imma* structure to become stable with respect to the *I*4/*mcm* structure. A schematic set of free energy curves representing this possibility is given in Figure 2b. A first order transition occurs between the *I*4/*mcm* and *Imma* structures at T_{tr}, between T_{c2} and T_{c1}, as might occur for $(b_2^* + b_2'^*) < 0$, $b_2^* > 0$, by analogy with the sequence for $BaTiO_3$ described by Devonshire (1949, 1951).

TABLE 5. Elastic constant variations expected in the stability field of a structure with *Pnma* symmetry ($q_2 \neq q_4 = q_6 \neq 0$, $q_1 = q_3 = q_5 = 0$), due to a transition from a parent cubic structure with $Pm\bar{3}m$ symmetry

$C_{11} = C_{11}^o - P^2\chi_2q_2^2 - 2M^2\chi_4q_4^2$	$C_{14} = -2M\lambda_5\chi_4q_4^2$
$C_{22} = C_{11}^o - O^2\chi_2q_2^2 - (M^2 + N^2)\chi_4q_4^2$	$C_{24} = C_{34} = -(M + N)\lambda_5\chi_4q_4^2$
$C_{33} = C_{11}^o - O^2\chi_2q_2^2 - (N^2 + M^2)\chi_4q_4^2$	$C_{56} = -\lambda_5^2\chi_5q_4^2$
$C_{12} = C_{12}^o - OP\chi_2q_2^2 - (M^2 + MN)\chi_4q_4^2$	$C_{44} = C_{44}^o + 2(\lambda_6 + \lambda_7)q_2^2 - 2\lambda_5^2\chi_4q_4^2$
$C_{13} = C_{12}^o - OP\chi_2q_2^2 - (MN + M^2)\chi_4q_4^2$	$C_{55} = C_{44}^o + 2\lambda_6q_2^2 - \lambda_5^2\chi_5q_4^2$
$C_{23} = C_{12}^o - O^2\chi_4q_2^2 - 2MN\chi_4q_4^2$	$C_{66} = C_{44}^o + 2\lambda_6q_2^2 - \lambda_5^2\chi_5q_4^2$

* $K_V = \frac{1}{3}\left(C_{11}^o + 2C_{12}^o\right) - 4\lambda_1^2\chi_2q_2^2 - 8\lambda_2^2\chi_4q_4^2$

* $G_V = \frac{1}{5}\left(C_{11}^o - C_{12}^o + 3C_{44}^o\right) - \frac{2}{5}\left(8\lambda_3^2\chi_2 + 3\lambda_6 + 2\lambda_7\right)q_2^2 - \frac{2}{5}\left(16\lambda_4^2\chi_4 + \lambda_5^2\chi_4 + \lambda_5^2\chi_5\right)q_4^2$

† $\chi_2^{-1} = \partial^2G/\partial q_2^2 = 2(b_1 + b_1')q_2^2 + 4(c_1 + c_1'')q_2^4 + 4\lambda_q'q_4^2$

† $\chi_4^{-1}\left(= \chi_6^{-1}\right) = \partial^2G/\partial q_4^2 = \left(2b_2 + 2b_2' + \frac{\lambda_5^2}{C_{44}^o}\right)q_4^2 + \left(10c_2 + \frac{19}{3}c_2''\right)q_4^4 + 2\lambda_q'q_2^2$

† $\chi_5^{-1} = \partial^2G/\partial q_5^2 = \left[\frac{\lambda_5^2}{C_{44}^o} + \frac{12\lambda_4^2}{\frac{1}{2}\left(C_{11}^o - C_{12}^o\right)} - b_2'\right]q_4^2 + \left(2c_2 + \frac{1}{3}c_2' - \frac{1}{3}c_2''\right)q_4^4 + 2\left(\lambda_q + \lambda_q'\right)\lambda_q'q_2^2$

Elastic constants, $C_{ik,c}$, for a unit cell with conventional orientation (**a**//X, **b**//Y, **c**//Z)

$C_{11,c} = \frac{1}{2}\left(C_{22} + C_{23}\right) + 2C_{24} + C_{44}$	$C_{23,c} = C_{12} - C_{14}$
$C_{22,c} = C_{11}$	$C_{44,c} = \frac{1}{2}\left(C_{55} + C_{66}\right) - C_{56}$
$C_{33,c} = \frac{1}{2}\left(C_{22} + C_{23}\right) - 2C_{24} + C_{44}$	$C_{55,c} = \frac{1}{2}\left(C_{22} - C_{23}\right)$
$C_{12,c} = C_{12} + C_{14}$	$C_{66,c} = \frac{1}{2}\left(C_{55} + C_{66}\right) + C_{56}$
$C_{13,c} = \frac{1}{2}\left(C_{22} + C_{23}\right) - C_{44}$	

* Expressions for the Voigt limits of bulk and shear modulus in terms of single-crystal elastic constants for an orthorhombic crystal were taken from Watt (1979).

† Values of q in the expressions for susceptibility are the equilibrium values given by Equations 37 and 38.

For both the situations represented in Figure 2, the equilibrium evolution of q_2 and q_4 in the *Pnma* structure is obtained by solving the simultaneous equations:

$$\frac{\partial G}{\partial q_2} = 0 = a_1\Theta_{s1}\left(\coth\left(\frac{\Theta_{s1}}{T}\right) - \coth\left(\frac{\Theta_{s1}}{T_{c1}}\right)\right) + \left(b_1^* + b_1'^*\right)q_2^2 + \left(c_1 + c_1''\right)q_4^4 + 4\lambda_q^*q_4^2 + \frac{2\lambda_5^2\left(\lambda_6 + \lambda_7\right)q_4^4}{C_{44}^{o\,2}} \quad (37)$$

$$\frac{\partial G}{\partial q_4} = 0 = 2a_2\Theta_{s2}\left(\coth\left(\frac{\Theta_{s2}}{T}\right) - \coth\left(\frac{\Theta_{s2}}{T_{c2}}\right)\right) + 2\left(2b_2^* + b_2'^*\right)q_2^2 + 4\left(2c_2 + c_2''\right)q_4^4 + 4\lambda_q^*q_2^2 + \frac{4\lambda_5^2\left(\lambda_6 + \lambda_7\right)q_2^2q_4^2}{C_{44}^{o\,2}}. \quad (38)$$

Expressions for the elastic constants of the *Pnma* structure are derived from Equation 1 in the same way as for the *I*4/*mcm*, *Imma*, and *P*4/*mbm* structures and are listed in Table 5. Elastic constants for the *Pnma* structure in its conventional orientation (**a**//X, **b**//Y, **c**//Z) have been obtained by rotation of axes, as before, and are included in Table 5 for completeness. Implicit in this treatment is the assumption that softening due to coupling of strains with each of the order parameter components is independent and additive. This is not necessarily the case if coupling between the M point and R point octahedral tilts is strong and occurs on a sufficiently rapid time scale that they behave effectively as a single tilt system. In this case, the relevant strain coupling coefficients would be for the combined strains that accompany the combined tilts and the relevant susceptibilities would be for the combined tilting mechanism.

TABLE 6. Final set of values for coefficients and other parameters in Equation 5, as used to calculate elastic and thermodynamic changes due to the $Pm\bar{3}m \rightarrow I4/mcm$ transition in $SrTiO_3$

a_2	0.6472 J/(mol·K)	0.0000180 GPa/K
Θ_{s2}	60.8 K	
T_{c2}	105.6 K	
$(b_2^* + b_2'^*)$	29.12 J/mol	0.000810 GPa
$(c_2 + c_2'')$	39.27 J/mol	0.001092 GPa
b_2^*		0.0012 GPa
$b_2'^*$		–0.00039 GPa
b_2		0.001152 GPa
b_2'		0.0000761 GPa
c_2		0.000912 GPa
c_2'		0.0033 GPa
c_2''		0.00018 GPa
λ_2		0.046 GPa
λ_4		–0.075 GPa
λ_5		0.125 GPa
C_{11}^0		332 GPa
C_{12}^0		104 GPa
C_{44}^0		124 GPa

CALIBRATION OF COEFFICIENTS FOR THE $Pm\bar{3}m \leftrightarrow I4/mcm$ TRANSITION IN $SrTiO_3$

Several authors have used experimental data from the literature to calibrate the coefficients in expressions for the elastic constants of $SrTiO_3$ (e.g., Slonczewski and Thomas 1970; Rehwald 1970a, 1970b, 1971; Lüthi and Moran 1970; Fossheim and Berre 1972). With the exception of Kityk et al. (2000a), the initial assumption has always been that the cubic → tetragonal transition can be described by a 24 Landau potential. In addition, attention has usually been focused only on the magnitude of the discontinuities at the transition point. A full analysis of the elastic constants of tetragonal $SrTiO_3$ over a wider temperature interval requires a new calibration. The sources of experimental data and the expressions used to extract values for specific coefficients are described in this section.

Order parameter evolution and calorimetry

Salje et al. (1998) and Hayward and Salje (1999) used various data from X-ray diffraction experiments, relating to the evolution of the order parameter, and high-resolution calorimetric data to calibrate the coefficients of a renormalized 246 potential for the R-point (Eq. 12). These are a_2, Θ_{s2}, T_{c2}, $(b_2^* + b_2'^*)$ and $(c_2 + c_2'')$. The values extracted by Hayward and Salje (1999) have been used here and are listed in Table 6. They are given in conventional SI units and in units of GPa (or GPa/K), the latter being obtained from the former by dividing by the molar volume of $SrTiO_3$. A molar volume of 3.595×10^{-5} m^3 has been used for the purposes of the present paper.

Bare elastic constants

The elastic constants of $SrTiO_3$ have been measured repeatedly by both ultrasonic and Brillouin methods in the past, but there is no single definitive data set. Different measurements from the literature have been assembled into a single coherent set here, for both the cubic and tetragonal structures, though this has required some rescaling according to how the data were originally presented. Hehlen et al. (1996) determined the velocities of acoustic modes in single domain samples of tetragonal $SrTiO_3$ by Brillouin spectroscopy. Values of velocity, v, from their Figures 2 and 4 have been converted to elastic constants here using $C_{ik} = \rho v^2$ and a value of the density, $\rho = 5.104$ Mg/m^3. Any errors introduced by using a single value for density, ignoring the effects of thermal expansion, are small in comparison with uncertainties in the raw velocity data. C_{33} and C_{44} were determined from data for longitudinal and transverse acoustic modes with propagation directions parallel to [001]. Values of C_{11} and C_{12} were obtained by combining data for the longitudinal mode [which depends on $\frac{1}{2}(C_{11} + C_{12} + 2C_{66})$] and a transverse mode [which depends on $\frac{1}{2}(C_{11} - C_{12})$] propagating in the [110] direction. In this context it was assumed that $C_{66} = C_{44}^0$, and $C_{44}^0 = 124$ GPa from below. Additional data of Hehlen et al. (1996) for C_{44} and C_{66} from a polydomain sample (their Fig. 1) were converted to units of GPa by applying a scaling factor that ensured close overlap with the first set of data for C_{44}.

Yamaguchi et al. (2002) gave their data only as Brillouin shifts. These have been converted to C_{ik} values by applying a scaling factor that gave close overlap of C_{44} in the stability field of the tetragonal structure with the values of C_{44} obtained from Hehlen et al. (1996). Some of the data of Yamaguchi et al. (2001, 2002) were obtained from samples enriched in ^{18}O. These authors concluded that the changes in acoustic mode frequencies associated with a change in $^{16}O/^{18}O$ content can be understood as being due to the change in density, at least for temperatures above ~30 K. Values of C_{ik} obtained from their ^{18}O-enriched samples have therefore been rescaled so as to give overlap of C_{44} with the data of Hehlen et al., as before. Hasebe et al. (2002, 2003) gave their experimental results, also for ^{18}O-enriched samples, as Brillouin shifts and these have been rescaled here to give values of C_{44}, which overlap with the values extracted from Hehlen et al. (1996). The data of Laubereau and Zurek (1970) were scaled in the same way.

Ultrasonic data of Bell and Rupprecht (1963), Lüthi and Moran (1970), Okai and Yoshimoto (1975), and Migliori et al. (1993) are in close agreement for C_{11} and C_{12} of cubic $SrTiO_3$. The results for C_{44} are slightly more scattered. Values for the same elastic constants given by Rehwald (1970a, 1970b, 1971, 1977) are systematically smaller by ~3%. The explanation of this difference is perhaps that Rehwald did not take any special measures "to eliminate losses and delays caused by the transducer and its bond" (Rehwald 1971, p. 23). For present purposes, therefore, all the elastic constants from Rehwald (1970a, 1970b, 1971, 1977) have been multiplied by 1.03. The data for C_{11} and C_{44} of cubic $SrTiO_3$ from Lei and Ledbetter (in Scott and Ledbetter 1997) were rescaled so as to overlap with the other ultrasonic data. In combination with the Brillouin data, a coherent picture of the elastic constants of $SrTiO_3$ over the temperature interval ~10–300 K is then obtained, as shown in Figure 3. The only exceptions are, first, for some of the ultrasonic data for C_{11} and C_{12} collected immediately below the cubic ↔ tetragonal transition point. In this range there is considerable scatter. The additional softening that the ultrasonic data show, in comparison with the Brillouin data, is almost certainly due to the influence of transformation twins (Rehwald 1971; Fossheim and Berre 1972; Scott 1999; Ang et al. 1999; Schranz et al. 1999; Kityk et al. 2000a, 2000b). Second, ^{18}O-enriched samples display an additional acoustic mode splitting below ~30 K, which has been interpreted in terms of a ferroelectric phase transition (Itoh et al. 1999; Yamaguchi et al. 2001, 2002; Yagi et al. 2002; Hasebe et al. 2002, 2003).

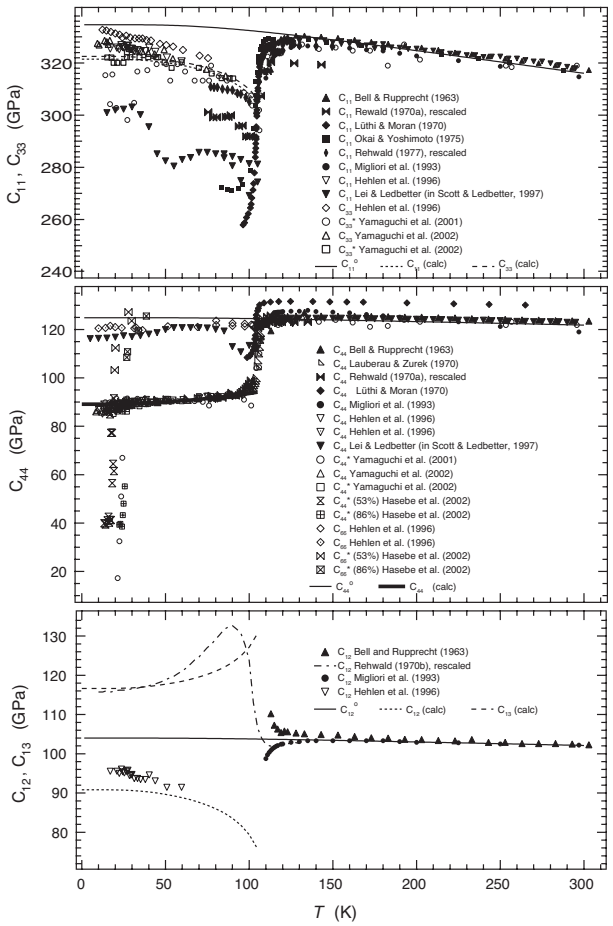

FIGURE 3. A complete set of elastic constants for $SrTiO_3$ assembled from the literature. Filled symbols represent ultrasonic data; open symbols represent Brillouin data. A star indicates that the data were obtained from ^{18}O-enriched $SrTiO_3$; the samples of Yamaguchi et al. (2001, 2002) were nominally pure $SrTi^{18}O_3$, while the samples of Hasebe et al. (2002) contained 86% ^{18}O and 53% ^{18}O. The data of Laubereau and Zurek (1970), Yamaguchi et al. (2001, 2002), and Hasebe et al. (2002) were scaled so that C_{44} overlapped closely with C_{44} data from Hehlen et al. (1996). Calculated variations of C_{11}, C_{33}, C_{12}, C_{13}, and C_{44} are from the Landau parameterization. Data for C_{12} from Rehwald (1970b) are shown as a continuous line, as in the original paper. The scatter in the data for C_{44} below ~30 K, as obtained from conversion of reported data for split acoustic modes directly to elastic constants, is due to additional structural changes which occur in ^{18}O-enriched samples.

The elastic constants of cubic $SrTiO_3$ show some weak temperature dependence, which is due to thermal expansion and normal non-linearities as $T \rightarrow 0$ K. Some softening ahead of the 106 K phase transition is also evident. For most of the calculations required here, no serious errors are introduced by assuming constant values of the bare elastic constants, but for the final calculation of the temperature-dependence of the tetragonal elastic constants it is necessary to include the variations of each of C_{11}^o, C_{12}^o, and C_{44}^o below 106 K. If the bare elastic constants scale approximately with the density of cubic $SrTiO_3$, a function of the form

$$C_{ik}^o = \frac{1}{A + B\Theta_s \coth\left(\frac{\Theta_s}{T}\right)} \quad (39)$$

should at least give a more or less appropriate leveling off as 0 K is approached. This is the inverse of the function usually used to describe volume evolution at low temperatures (see the section on spontaneous strain, below). Equation 39 was fit to C_{11} (data of Okai and Yoshimoto 1975), C_{12} (data of Migliori et al. 1993), and C_{44} (data of Yamaguchi et al. 2001) in the temperature intervals 215–288, 180–297, and 202–296 K, respectively, with Θ_s fixed at the value (128 K) obtained below from the lattice parameters of the cubic structure. The fit parameters are A = 0.002870, 0.009496, 0.007871, $B = 9.257 \times 10^{-7}$, 9.332×10^{-7}, 1.058×10^{-6} GPa^{-1}, respectively. The fits themselves are shown as solid lines in Figure 3. The fit values at 106 K have been selected to represent the bare elastic constants of cubic $SrTiO_3$ in calculations of elastic softening due to the phase transition: $C_{11}^o = 332$, $C_{12}^o = 104$, $C_{44}^o = 124$ GPa (Table 6).

Softening of the bare elastic constants as $T \rightarrow T_c$ from above is commonly observed even for phase transitions that are not driven by the softening of an acoustic mode. Critical fluctuations and defects could cause changes to the elastic properties in the close vicinity of the transition point but softening over a wider temperature interval (greater than a few degrees) has been explained in terms of fluctuations due to interactions between modes with k-vectors just away from the critical point of the Brillouin zone (Höchli 1972; Rehwald 1973; Cummins 1979; Lüthi and Rehwald 1981; Yao et al. 1981; Fossum 1985; Carpenter and Salje 1998). This softening is usually described by an expression of the form

$$\Delta C_{ik} = A_{ik}|T - T_c|^K. \quad (40)$$

ΔC_{ik} is the difference between the observed values of C_{ik} and values of the appropriate bare elastic constants extrapolated from high temperatures. A_{ik} is a property of the material, while K is expected to have values between –1/2 and –2, depending on the anisotropy and dispersion of soft branches around the critical point (Axe and Shirane 1970; Pytte 1970, 1971; Höchli 1972; Carpenter and Salje 1998). For a cubic crystal this mechanism is expected to apply only to C_{11} and C_{12}, with $\Delta C_{11} = \Delta C_{12}$. Differences between calculated values of C_{12}^o and the C_{12} data of Migliori et al. (1993) have been used here to obtain $\Delta C_{12} = 30.17(T–T_{c2})^{-1.20}$, with T_{c2} set at 105.6 K. The value of K is slightly smaller than that given by Carpenter and Salje (1998) because a non-linear fit to C_{12}^o at high temperatures has been used. The same variation was assumed for ΔC_{11}. Due to symmetry constraints, C_{44} does not soften by the same mechanism and its observed softening is indeed restricted to a narrower temperature interval. Equation 40 has nevertheless been used to provide an empirical description of the data of Yamaguchi et al. (2001), $\Delta C_{44} = 8.7(T–T_{c2})^{-0.80}$. These parameters are needed below for calculations of the bulk and shear moduli of cubic $SrTiO_3$ so as to reflect, at least semi-quantitatively, the observed softening of the individual elastic constants above T_{c2}.

Stress dependence

External application of hydrostatic pressure or non-hydrostatic stress results in significant changes to the critical temperature, T_{c2}, and to the structural evolution of $SrTiO_3$. Experimental data

from the literature have been used in the past to extract values for some of the Landau parameters, therefore (Pietrass and Hegenbarth 1969; Laubereau and Zurek 1970; Slonczewski 1970; Lüthi and Moran 1970; Müller et al. 1970; Slonczewski and Thomas 1970; Rehwald 1970a, 1971; Burke et al. 1971; Fossheim and Berre 1972; Okai and Yoshimoto 1975). A review of these data is presented here as part of the process of determining a full set of internally consistent coefficients.

Following the usual convention that a compressive stress has negative sign and tensile stress has positive sign, the contribution to the excess free energy due to the application of stresses, σ_i, is $-\sum_{i=1-6} e_i\sigma_i$. This term can be added directly to the Landau expansions (Slonczewski 1970; Müller et al. 1970; Burke et al. 1971; Fossheim and Berre 1972). Making use of symmetry-adapted forms of the strain, the 246 Landau expansion for cubic ↔ tetragonal $SrTiO_3$ becomes

$$\begin{aligned}G = {} & \frac{1}{2}a_2\Theta_{s2}\left(\coth\left(\frac{\Theta_{s2}}{T}\right)-\coth\left(\frac{\Theta_{s2}}{T_{c2}}\right)\right)\left(q_4^2+q_5^2+q_6^2\right)+\frac{1}{4}b_2\left(q_4^2+q_5^2+q_6^2\right)^2\\ & +\frac{1}{4}b_2'\left(q_4^4+q_5^4+q_6^4\right)+\frac{1}{6}c_2\left(q_4^2+q_5^2+q_6^2\right)^3+\frac{1}{6}c_2'\left(q_4q_5q_6\right)^2\\ & +\frac{1}{6}c_2''\left(q_4^2+q_5^2+q_6^2\right)\left(q_4^4+q_5^4+q_6^4\right)+\lambda_2e_a\left(q_4^2+q_5^2+q_6^2\right)\\ & +\lambda_4\left[\sqrt{3}e_o\left(q_5^2-q_6^2\right)+e_t\left(2q_4^2-q_5^2-q_6^2\right)\right]+\lambda_5\left(e_4q_4q_6+e_5q_4q_5+e_6q_5q_6\right)\\ & +\frac{1}{4}\left(C_{11}^o-C_{12}^o\right)\left(e_o^2+e_t^2\right)+\frac{1}{6}\left(C_{11}^o+2C_{12}^o\right)e_a^2+\frac{1}{2}C_{44}^o\left(e_4^2+e_5^2+e_6^2\right)\\ & +P_ae_a+P_oe_o+P_te_t-\sigma_4e_4-\sigma_5e_5-\sigma_6e_6,\end{aligned} \tag{41}$$

where

$$P_a=-\frac{1}{3}\left(\sigma_1+\sigma_2+\sigma_3\right) \tag{42}$$

$$P_o=-\frac{1}{2}\left(\sigma_1-\sigma_2\right) \tag{43}$$

$$P_t=-\frac{1}{2\sqrt{3}}\left(2\sigma_3-\sigma_1-\sigma_2\right). \tag{44}$$

Substituting for the strains and regrouping terms gives

$$\begin{aligned}G = {} & \frac{1}{2}a_2\Theta_{s2}\left(\coth\left(\frac{\Theta_{s2}}{T}\right)-\coth\left(\frac{\Theta_{s2}}{T_{c2}}\right)\right)\left(q_4^2+q_5^2+q_6^2\right)+\frac{1}{4}b_2^*\left(q_4^2+q_5^2+q_6^2\right)^2\\ & +\frac{1}{4}b_2'^*\left(q_4^4+q_5^4+q_6^4\right)+\frac{1}{6}c_2\left(q_4^2+q_5^2+q_6^2\right)^3+\frac{1}{6}c_2'\left(q_4q_5q_6\right)^2\\ & +\frac{1}{6}c_2''\left(q_4^2+q_5^2+q_6^2\right)\left(q_4^4+q_5^4+q_6^4\right)-\frac{\lambda_2\left(q_4^2+q_5^2+q_6^2\right)P_a}{\frac{1}{3}\left(C_{11}^o+2C_{12}^o\right)}-\frac{\sqrt{3}\lambda_4\left(q_5^2-q_6^2\right)P_o}{\frac{1}{2}\left(C_{11}^o-C_{12}^o\right)}\\ & -\frac{\lambda_4\left(2q_4^2-q_5^2-q_6^2\right)P_t}{\frac{1}{2}\left(C_{11}^o-C_{12}^o\right)}+\frac{\lambda_5\left(\sigma_4q_4q_6+\sigma_5q_4q_5+\sigma_6q_5q_6\right)}{C_{44}^o}.\end{aligned} \tag{45}$$

There are other terms in P_a, P_o, and P_t that arise in this process, but they do not include the order parameter. They do not contribute to the excess free energy associated with a phase transition, therefore, and have been left out of Equation 45.

Hydrostatic pressure

Hydrostatic pressure, P (= P_a) causes a renormalization of the second order term such that the transition pressure occurs (for a thermodynamically continuous transition) when

$$\coth\left(\frac{\Theta_{s2}}{T}\right)-\coth\left(\frac{\Theta_{s2}}{T_{c2}}\right)-\frac{2\lambda_2P_{a,c}}{a_2\Theta_{s2}\frac{1}{3}\left(C_{11}^o+2C_{12}^o\right)}=0, \tag{46}$$

where $P_{a,c}$ is the transition pressure at a given temperature. Thus,

$$P_{a,c}=\frac{a_2\Theta_{s2}\frac{1}{3}\left(C_{11}^o+2C_{12}^o\right)}{2\lambda_2}\left(\coth\left(\frac{\Theta_{s2}}{T}\right)-\coth\left(\frac{\Theta_{s2}}{T_{c2}}\right)\right). \tag{47}$$

Data for the pressure dependence of the cubic ↔ tetragonal transition in $SrTiO_3$ are reproduced from Okai and Yoshimoto (1975) in Figure 4a. Equation 47 cannot be fit to the data using a constant value of the coupling coefficient λ_2. Taken at face value, the experimental data show a break in slope at ~1 GPa. Fitting with two separate straight lines gives an extrapolated value of 5.9 GPa for P_c at 295 K (Fig. 4a). This compares with room temperature values of 6.0 GPa given by Grzechnik et al. (1997) and 6.4 GPa given by Ishidate and Isonuma (1992). The implication is that the structural evolution of $SrTiO_3$ at low pressures is different from the evolution at high pressures, probably through variations in the strength of coupling between the volume strain and q_4^2. For present purposes a constant value of $\lambda_2 = 0.046$ GPa has been obtained from a fit to all the data shown in Figure 4a (broken line), with the values of a_2, Θ_{s2}, T_{c2} and $1/3(C_{11}^o + 2C_{12}^o)$ as listed in Table 6. This fit is equivalent to $dP_{a,c}/dT = 0.034$ GPa/K, which compares with 0.067 GPa/K given previously by Sorge et al. (1970).

Stress applied parallel to [111]

When a compressive stress, P_{111}, is applied parallel to [111] of cubic $SrTiO_3$ a small rhombohedral strain, $e_4 = e_5 = e_6 \neq 0$, is induced. This pseudo-cubic structure becomes more markedly rhombohedral above a critical stress, $P_{111,c}$ (Müller et al. 1970). P_{111} is equivalent to a stress tensor, which has

$$-\sigma_1 = -\sigma_2 = -\sigma_3 = -\sigma_4 = -\sigma_5 = -\sigma_6 = {}^1/_3P_{111}. \tag{48}$$

The transition point is then given, for the case of a continuous phase transition, by

$$P_{111,c}=\frac{3a_2\Theta_{s2}}{2}\left(\frac{\frac{1}{3}\left(C_{11}^o+2C_{12}^o\right)C_{44}^o}{\lambda_2C_{44}^o+\lambda_5\frac{1}{3}\left(C_{11}^o+2C_{12}^o\right)}\right)\left(\coth\left(\frac{\Theta_{s2}}{T}\right)-\coth\left(\frac{\Theta_{s2}}{T_{c2}}\right)\right) \tag{49}$$

to a good approximation. Data from Müller et al. (1970) and Burke and Pressley (1969) for the stability limits of different structural states of $SrTiO_3$ as a function of P_{111} are reproduced in Figure 4b. A fit of Equation 49 to the data for the pseudo-cubic ↔ $R\bar{3}c$ transition gives $\lambda_5 = 0.07 \pm 0.02$ GPa, using values for the other coefficients listed in Table 6. T_{c2} was allowed to vary and the best-fit value was 102.2 ± 1 K.

If the P_{111} stress is applied to tetragonal $SrTiO_3$, the crystals become monoclinic. In crystallographic terms, a [111] stress causes the axis of the octahedral tilt to rotate from [001] for the $I4/mcm$ structure toward [111] for the $R\bar{3}c$ structure. When the tilt lies between these limits the crystal has $C2/c$ symmetry, as characterized by the order parameter components $q_4 = q_6 \neq q_5 \neq 0$. Note that, in this description, the tetragonal structure has $q_4 = q_6 = 0$, $q_5 \neq 0$ at zero stress, i.e., it is a different twin orientation

from $q_4 \neq 0$. This orientation is used throughout this section. Following the approach of Slonczewski (1970), the monoclinic ↔ rhombohedral transition point, $P_{111,t}$, is obtained by calculating the excess free energies of each of these phases. The excess free energy of the $C2/c$ structure is given by Equation 45 with $P_a = -\sigma_4 = -\sigma_5 = -\sigma_6 = {}^1/_3 P_{111}$:

$$G = \frac{1}{2}a_2\Theta_{s2}\left(\coth\left(\frac{\Theta_{s2}}{T}\right) - \coth\left(\frac{\Theta_{s2}}{T_{c2}}\right)\right)\left(2q_4^2 + q_5^2\right) + \frac{1}{4}b_2^*\left(2q_4^2 + q_5^2\right)^2 + \frac{1}{4}b_2^{'*}\left(2q_4^4 + q_5^4\right) + \frac{1}{6}c_2\left(2q_4^2 + q_5^2\right)^3 + \frac{1}{6}c_2^{'}\left(q_4^2 q_5\right)^2 + \frac{1}{6}c_2^{''}\left(2q_4^2 + q_5^2\right)\left(2q_4^4 + q_5^4\right) - \frac{\lambda_2 P_{111}}{\left(C_{11}^o + 2C_{12}^o\right)}\left(2q_4^2 + q_5^2\right) - \frac{\lambda_5 P_{111}}{3C_{44}^o}\left(q_4^2 + 2q_4 q_5\right). \quad (50)$$

Equilibrium values of the order parameter components at different P_{111} and T are then given by solutions to the simultaneous equations

$$\frac{\partial G}{\partial q_4} = 0 = a_2\Theta_{s2}\left(\coth\left(\frac{\Theta_{s2}}{T}\right) - \coth\left(\frac{\Theta_{s2}}{T_{c2}}\right)\right)q_4 + b_2^*\left(2q_4^2 + q_5^2\right)q_4 + b_2^{'*}q_4^3 + c_2\left(2q_4^2 + q_5^2\right)^2 q_4 + \frac{1}{3}c_2^{'}q_4^3 q_5^2 + \frac{1}{3}c_2^{''}\left(6q_4^5 + 2q_4^3 q_5^2 + q_4 q_5^4\right) - \frac{2\lambda_2 P_{111}}{\left(C_{11}^o + 2C_{12}^o\right)}q_4 - \frac{\lambda_5 P_{111}}{3C_{44}^o}\left(q_4 + q_5\right) \quad (51)$$

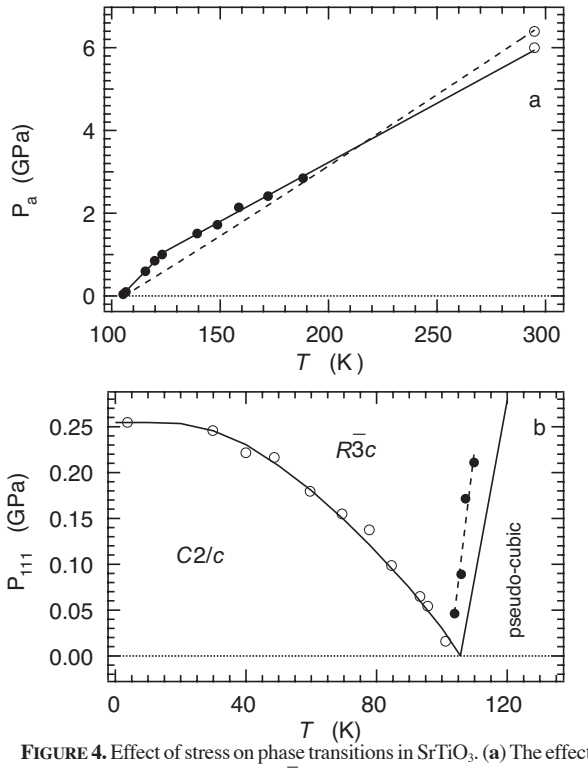

FIGURE 4. Effect of stress on phase transitions in $SrTiO_3$. (**a**) The effect of hydrostatic pressure, P_a, on the $Pm\bar{3}m \leftrightarrow I4/mcm$ transition: filled circles are data from Okai and Yoshimoto (1975); open circles are data of Ishidate and Isonuma (1992) and Grzechnik et al. (1997). The broken line is a fit of Equation 47 to all the data combined. Solid lines are separate fits to data from room pressure to 1 GPa and from 1 to 2.85 GPa. The latter fit has been extrapolated to 295 K. (**b**) Data from Müller et al. (1970) for the effect of stress applied parallel to [111]. The broken line is a fit of Equation 49 to the data of Müller et al. (1970) for the pseudo-cubic ↔ rhombohedral transition. The solid straight line is the calculated variation of $P_{111,c}$ for the same transition using Equation 49 and values of parameters as given in Table 6. The curved line links values calculated for the transition stress, $P_{111,t}$, for the monoclinic ↔ rhombohedral transition. Note that the crystals of Müller et al. (1970) had $T_{c2} \approx 102.2$ K, whereas $T_{c2} = 105.6$ K has been used for the present calculations.

$$\frac{\partial G}{\partial q_5} = 0 = a_2\Theta_{s2}\left(\coth\left(\frac{\Theta_{s2}}{T}\right) - \coth\left(\frac{\Theta_{s2}}{T_{c2}}\right)\right)q_5 + b_2^*\left(2q_4^2 + q_5^2\right)q_5 + b_2^{'*}q_5^3 + c_2\left(2q_4^2 + q_5^2\right)^2 q_5 + \frac{1}{3}c_2^{'}q_4^4 q_5 + \frac{1}{3}c_2^{''}\left(2q_4^4 q_5 + 4q_4^2 q_5^3 + 3q_5^5\right) - \frac{2\lambda_2 P_{111}}{\left(C_{11}^o + 2C_{12}^o\right)}q_5 - \frac{2\lambda_5 P_{111}}{3C_{44}^o}q_4. \quad (52)$$

Numerical solutions have been obtained for Equations 51 and 52, using values of the coefficients listed in Table 6 and the software package Mathematica. If b_2^* and $b_2^{'*}$ are extracted from spectroscopic data (see below), the only unknown parameter is $c_2^{'}$. Trial values for this coefficient were applied until the value of the transition points, $P_{111,t}$, at 4.2 and 78 K corresponded to the experimental values determined by Müller et al. (1970). However, there was no single value of $c_2^{'}$ derived for these values of b_2^* and $b_2^{'*}$ which matched the experimental transition points simultaneously. Trial values of b_2^* and $b_2^{'*}$ were therefore applied, with iterations of λ_5 and $c_2^{''}$ to match C_{44}, as described below. The final fit has $b_2^* = 0.0012$ and $b_2^{'*} = -0.00039$, with $c_2^{'} = 0.0033$, which are taken here as the preferred values for these coefficients (Table 6). It is interesting to note that the experimental data of Müller et al. give $dP_{111,c}/dT = 0.029 \pm 0.005$ GPa/K, ($dT/dP_{111,c} \approx 35 \pm 6$ K), which is matched by a calculated slope of 0.024 GPa/K (~41 K/GPa), if the volume/order parameter coupling coefficient λ_2 is zero (with $\lambda_5 = 0.125$ GPa). A value of $\lambda_2 = 0.046$ GPa gives the slope shown in Figure 4b (0.019 GPa/K, ~53 K/GPa). Thus, allowing λ_2 to vary from rather small values at low temperatures to larger values at high temperatures would permit better agreement to be obtained between experimental and calculated variations for both $P_{a,c}$ and $P_{111,c}$.

Values of q_4 and q_5 from the solutions to Equations 51 and 52, using the final set of coefficients, have been used to calculate the free energies of the monoclinic and rhombohedral structures, as shown in Figure 5a. With increasing magnitude of P_{111}, the monoclinic structure evolves across order parameter space from the tetragonal starting point toward the rhombohedral structure. The numerical solutions suggest that the approach toward $R\bar{3}c$ symmetry may be asymptotic. This point was not explored in detail but if the transition is first order in character, as discussed by Slonczewski (1970) and Müller et al. (1970), the discontinuity at the transition point is small. There are actually four solutions to the simultaneous equations (51 and 52). In addition to the rhombohedral, monoclinic/pseudo-orthorhombic ($q_4 = q_6 =$ large, $q_5 =$ small), and monoclinic/pseudo-tetragonal ($q_4 = q_6 =$ small, $q_5 =$ large) structures, an unexpected monoclinic structure was found with $q_4 = q_6$ and q_5 similar in magnitude to q_4 but opposite in sign. The pseudo-orthorhombic structure is, as expected, always intermediate in energy between the rhombohedral and pseudo-tetragonal structures (Fig. 5a). The additional monoclinic phase has the highest energy for most values of P_{111}.

Values of $P_{111,t}$ were calculated at ~10 K intervals below T_{c2} using the final set of parameters listed in Table 6. They show close agreement with the experimental data of Müller et al. (1970), bearing in mind that the transition point at zero stress for the sample used by Müller et al. was ~102 K (Fig. 4b). There are further experimental data for the effect of stress parallel to [111] at 4.2 K (Burke and Pressley 1969), 78 K and T_c + 1.8 K (Müller et al. 1970), which allow a final comparison of observed and calculated variations of the order parameter. Burke and Pressley (1969) measured the fluorescence of Cr^{3+} impurities in $SrTiO_3$

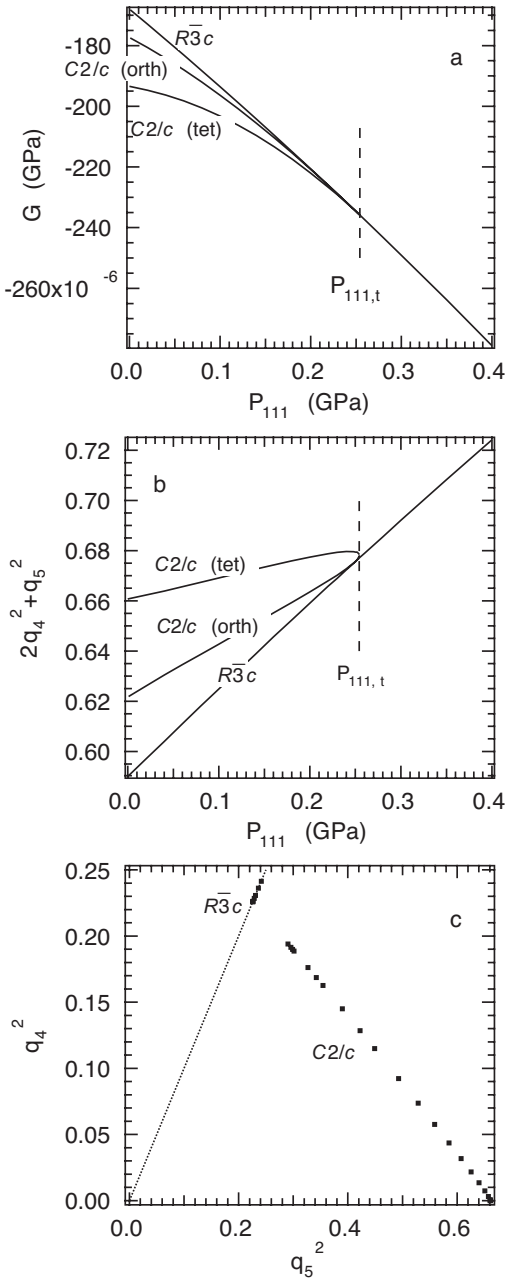

FIGURE 5. Results of calculations at 4.2 K for the stability of pseudo-tetragonal, pseudo-orthorhombic (both actually monoclinic, $C2/c$) and rhombohedral structures with increasing stress applied parallel to [111]. Note that, for these calculations, the stable tetragonal structure at zero stress has $q_5 \neq 0$, rather than $q_4 \neq 0$; i.e., it is a different twin orientation from that used elsewhere in this paper. (**a**) The free energies of the three structures appear to asymptote toward a single value at the $C2/c \leftrightarrow R\bar{3}c$ transition point, $P_{111,t}$. (**b**) The sum of squares of the three components of the order parameter also appear to converge but details of the topology very close to $P_{111,t}$ were not explored. (**c**) The tetragonal structure at zero stress has $q_5^2 = 0.661$ but then evolves across order parameter space toward the $R\bar{3}c$ structure. The last point calculated for the $C2/c$ structure and the first point for the $R\bar{3}c$ structure differ by 0.001 GPa.

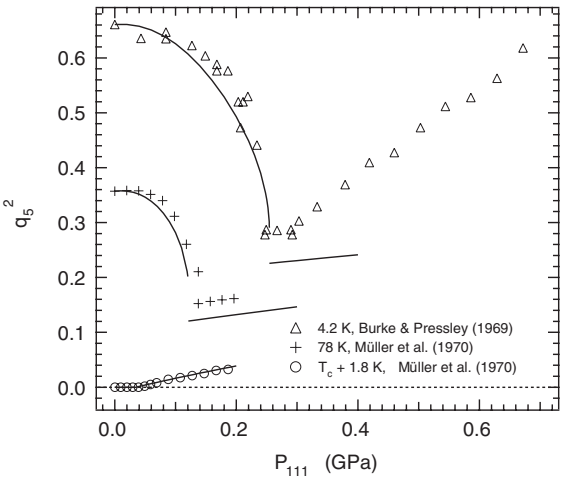

FIGURE 6. Variation of experimental and calculated values for q_5^2 with increasing stress parallel to the [111] axis. (For the calculations involving [111] stress, the $I4/mcm$ structure has an orientation with $q_5 \neq 0, q_4 = q_6 = 0$). The experimental values were derived from spectroscopic data calibrated against the order parameter for tetragonal $SrTiO_3$ at zero stress. The calculated values are from Equations 51 and 52 using values of coefficients listed in Table 6. The experimental data from Müller et al. (1970) from above T_c were collected at 104 K for a sample with $T_{c2} = 102.2$ K; the calculated values are therefore for $T_{c2} + 1.8$ K = 107.4 K. The patterns of calculated variations are similar to the observed patterns, but the actual values are systematically smaller for the rhombohedral structure. Above $P_{111} \approx 0.3$ GPa, the observed variation at 4.2 K is steeper than the calculated variation.

as a function of P_{111}. The splitting, Δ, of a doublet centered at ~12 600 cm^{-1} varies as a function of temperature (Stokowski and Schawlow 1969) in a manner that is consistent with $\Delta \propto q_5^2$ for the tetragonal structure. The data of Burke and Pressley for Δ as a function of P_{111} at 4.2 K have therefore been used to estimate the evolution of the order parameter by calibrating the value of Δ at $P_{111} = 0$ with the value of q_5^2 at 4.2 K given by Equation 15 ($q_5^2 = 0.2237\Delta$). Müller et al. (1970) used the splitting, ΔH, of lines in EPR spectra from Fe^{3+} with a nearest neighbor oxygen vacancy to follow the octahedral rotations in a similar manner. Scaling the octahedral rotation angle, ϕ, with the order parameter at 78 K for zero stress and using their calibration for ϕ in terms of ΔH gave a calibration $q_5^2 = 0.0000619\,\Delta H^2$ for data collected at 104 K. The 78 K data of Müller et al. (1970) were scaled as $q_5^2 = 0.357(\Delta H/\Delta H_o)^2$. (The spectroscopic parameters were given with respect to the value at zero stress, ΔH_o, and $q_5^2 = 0.357$ at 78 K). Figure 6 shows a comparison of the final "experimental" variation of q_5^2 with the calculated variations. For the highest temperature data set, values were calculated at $T_{c2} + 1.8$ K = 107.4 K. There is qualitative agreement but the calculated values are smaller than the experimental values for the rhombohedral structure. The calculated variations of q_5^2 were insensitive to the choice of values for the parameters b_2^*, $b_2'^*$ (at constant $b_2^* + b_2'^*$), λ_5 and c_2'. On the other hand, rescaling the "experimental" values of q_5^2 for the rhombohedral structure by a further factor of ~0.8 produces much closer agreement. Perhaps the scaling for q_5^2 with respect to spectroscopic data differs between the tetragonal and trigonal phases.

There are additional data in the literature for the effect of [111] stress on the soft mode frequencies (e.g., Burke et al. 1971) but, in

view of doubts over the conventional soft mode model discussed below for describing soft mode frequencies as a function of temperature, these have not been examined in the present context.

Biaxial stress

Fossheim and Berre (1972) devised an experimental rig to apply a compressive stress simultaneously parallel to [100] and [010] of cubic $SrTiO_3$. This stress induces a small tetragonal strain but, at some critical stress, the crystal transforms to the *I*4/*mcm* structure. If the magnitude of the stress is P_{bia}, the critical stress, $P_{bia,c}$, can be found by substituting $-\sigma_1 = -\sigma_2 = P_{bia}$ into Equations 42–45. This leads to

$$P_{bia,c} = \frac{3a_2\Theta_{s2}}{2}\left(\frac{\frac{1}{3}\left(C_{11}^o + 2C_{12}^o\right)\cdot\frac{1}{2}\left(C_{11}^o - C_{12}^o\right)}{2\lambda_2\frac{1}{2}\left(C_{11}^o - C_{12}^o\right) - 2\sqrt{3}\lambda_4\frac{1}{3}\left(C_{11}^o + 2C_{12}^o\right)}\right)\left(\coth\left(\frac{\Theta_{s2}}{T}\right) - \coth\left(\frac{\Theta_{s2}}{T_{c2}}\right)\right). \quad (53)$$

The experimental value of $dT/dP_{bia,c}$ given by Fossheim and Berre (1972) is 92 ± 3 K/GPa. The calculated slope obtained by substitution of values of λ_2, λ_4, C_{11}^o, C_{12}^o, and Θ_s from Table 1 into Equation 53 is 115 K/GPa. Setting $\lambda_2 = 0$ gives a slope of 93 K/GPa, implying that some temperature or stress dependence of λ_2 could account, at least in part, for the discrepancy between observed and calculated values.

The effect of a stress parallel to [100] is expected to be half that for P_{bia}, but Fossheim and Berre obtained a value of only 36 K/GPa for the slope of the transition temperature as a function of applied stress. They surmised that the discrepancy could have been due to the influence of twin domains when a [100] stress is applied. In this context, it is worth noting that the substantial elastic softening due to twin wall motions under non-hydrostatic stress observed by Schranz et al. (1999), Kityk et al. (2000a, 2000b), and Harrison et al. (2003) was recorded at applied stresses that were generally below those used in the early studies of stress-induced transitions. The expectation is that, by the time large stresses are achieved, single crystals are reduced to only one twin domain or the twin walls have moved to fixed positions from which they do not move further.

Spontaneous strain

Hayward and Salje (1999) used the dilatometric data of Liu et al. (1997) to determine the tetragonal strain in $SrTiO_3$ below T_{c2}, but not the volume strain. The data from Figure 1 of Liu et al. have therefore been re-examined in somewhat more detail. To these have been added the data from Figure 1 of Okazaki and Kawaminami (1973) for cubic $SrTiO_3$. Values of dilatation parallel to a and c of the tetragonal structure and parallel to a of the cubic structure from Liu et al. were scaled to $a = 3.89846$ Å at 110 K (from Sato et al. 1985). The cubic parameters of Okazaki and Kawaminami were rescaled slightly so as to overlap closely with these (Fig. 7a). A baseline, a_o, was then fit to the data for cubic $SrTiO_3$ using the commonly used function (e.g., Meyer et al. 2000, 2001; Sondergeld et al. 2000; Carpenter et al. 2003; after Salje et al. 1991a) which accounts for normal third law saturation as $T \rightarrow 0$ K,

$$a_o = a_c + a_s\Theta_s\coth\left(\frac{\Theta_s}{T}\right). \quad (54)$$

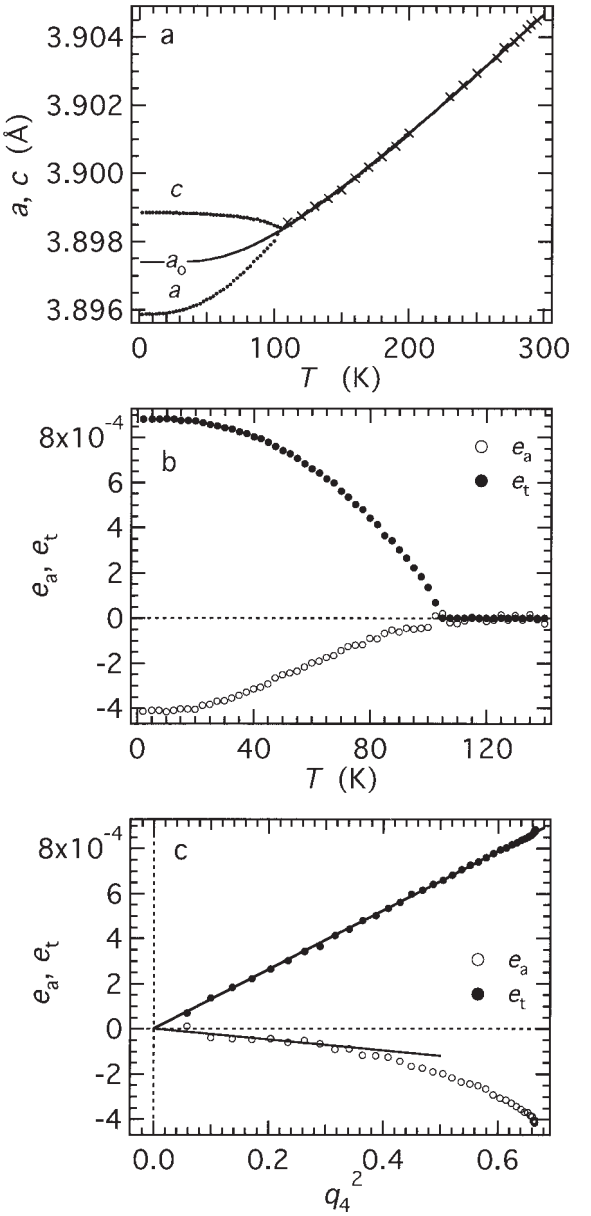

FIGURE 7. Spontaneous strain variations. (**a**) Data for tetragonal and cubic $SrTiO_3$, extracted at 2.5 K intervals up to 200 K, are from Liu et al. (1997); data for cubic $SrTiO_3$ up to 300 K (crosses) are from Okazaki and Kawaminami (1973). The former were scaled to give $a = 3.89846$ Å at 110 K and the latter were scaled to produce close overlap above 106 K. The solid line is a fit to the combined cubic data using Equation 54 with a_c fixed at 3.8925 Å. (**b**) Variations of the tetragonal (e_t) and volume (e_a) strains with temperature. (**c**) The tetragonal strain is a linear function of q_4^2 from Equation 15 with values of the coefficients as listed in Table 6, and the slope is 0.001311 ± 0.000002. The volume strain is a non-linear function of q_4^2; for the temperature interval 80–105 K, the straight line has $\lambda_2 = 0.043$ GPa.

A fit to the combined cubic data yielded $a_c = 3.8919$ Å, $a_s = 3.977 \times 10^{-5}$ Å, and $\Theta_s = 142.7$ K.

Individual strains due to the phase transition were calculated using the usual relations $e_1 = e_2 = (a - a_o)/a_o$, $e_3 = (c - a_o)/a_o$ and then converted to the symmetry-adapted forms given above

(Eqs. 2 and 4). The slope of e_t against q_4^2 gives $\lambda_4 = -0.075$ (± 0.0001) GPa for $1/2(C_{11}^\circ - C_{12}^\circ) = 114$ GPa (Eq. 8). This is the preferred value for present purposes because its determination is independent of the choice of value for λ_2. It is also insensitive to the choice of baseline, a_o.

The variation of e_a is a distinctly non-linear function of q_4^2. A straight line fit to the data in the interval 80–105 K gave a value of $\lambda_2 = 0.084 \pm 0.004$ GPa, for $1/3(C_{11}^\circ + 2C_{12}^\circ) = 180$ GPa. This is greater than the value obtained above from the pressure dependence of the transition temperature, probably as a result of the large uncertainties in extrapolating a_o below 106 K. Small adjustments were therefore made iteratively to the fit for a_o, using trial values of a_c. A value of $\lambda_2 = 0.043$ was obtained from $a_c = 3.8925$, $a_s = 3.828 \times 10^{-5}$ Å, $\Theta_s = 128.1$ K. These parameters were used to calculate the variations of a_o and e_a shown in Figure 7. Such adjustments always gave non-linear variations of e_a with q_4^2, and this result is further suggestive of some temperature dependence for λ_2.

Soft mode frequencies

The conventional view of phase transitions driven by a soft mode is that the frequency of the soft mode is related to the inverse susceptibility of the order parameter. For R point transitions in perovskites, the normal starting point for analyzing this relationship has been a 24 potential with terms grouped in a slightly different way (Thomas and Müller 1968; Harley et al. 1973)

$$G = \frac{1}{2}A\left(T - T_{c2}\right)\left(q_4^2 + q_5^2 + q_6^2\right) + \frac{1}{4}B\left(q_4^4 + q_5^4 + q_6^4\right) + \frac{1}{2}C\left(q_4^2q_5^2 + q_5^2q_6^2 + q_4^2q_6^2\right), \quad (55)$$

where

$$B = b_2^* + b_2^{'*} = b_2 + b_2^{'} - \frac{2\lambda_2^2}{\frac{1}{3}\left(C_{11}^o + 2C_{12}^o\right)} - \frac{8\lambda_4^2}{\frac{1}{2}\left(C_{11}^o - C_{12}^o\right)} \quad (56)$$

$$C = b_2^* = b_2 - \frac{\lambda_5^2}{C_{44}^o} - \frac{2\lambda_2^2}{\frac{1}{3}\left(C_{11}^o + 2C_{12}^o\right)} + \frac{4\lambda_4^2}{\frac{1}{2}\left(C_{11}^o - C_{12}^o\right)}. \quad (57)$$

The soft mode above T_{c2}, with F_{2u} symmetry, splits into two separate modes below T_{c2}, with A_{1g} and E_g symmetry. The frequencies of the two soft modes in the *I*4/*mcm* stability field are ω_A and ω_E, and are expected to vary proportionately to the eigenvalues of the inverse susceptibility matrix, $\chi_{ik}^{-1} = \partial^2 G/\partial q_i \partial q_k$ (Thomas and Müller 1968). For *I*4/*mcm* symmetry, the inverse susceptibility is given by double differentiation of Equation 12 followed by setting $q_5 = q_6 = 0$, to give

$$\omega_A^2 \propto \frac{\partial^2 G}{\partial q_4^2} = 2\left(b_2^* + b_2^{'*}\right)q_4^2 + 4\left(c_2 + c_2^{''}\right)q_4^4 \quad (58)$$

$$\omega_E^2 \propto \frac{\partial^2 G}{\partial q_5^2} = \frac{\partial^2 G}{\partial q_6^2} = -b_2^{'*}q_4^2 - \frac{2}{3}c_2^{''}q_4^4, \quad (59)$$

where q_4 is the equilibrium value of the order parameter. For a 24 potential, the expectation is that the square of the soft mode frequency should scale with q_4^2, and the ratio of the squared values

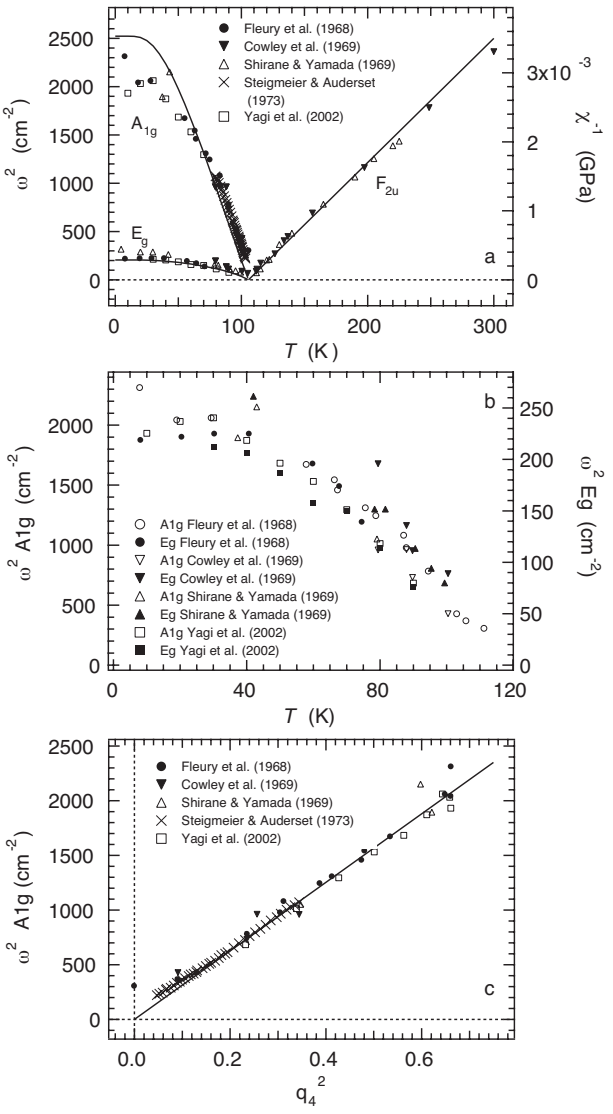

FIGURE 8. Soft mode frequency data for $SrTiO_3$ from the literature. The temperatures of data from Cowley et al. (1969) and Fleury et al. (1968) were rescaled so as to give $T_{c2} \approx 106$ K instead of ~110 K. Data of Yagi et al. (2002) are for a sample with 87% ^{18}O. (**a**) Frequency squared (left axis) compared with calculated susceptibilities (solid lines, Eqs. 62–64, right axis). (**b**) ω_A^2 and ω_E^2 show the same variation with temperature as each other, consistent with $\omega_A^2 \propto \omega_E^2 \propto q_4^2$. (**c**) Within reasonable experimental uncertainties, ω^2 for the A_{1g} mode scales linearly with calculated values of q_4^2. The straight line is a guide to the eye.

of the soft mode frequencies would be

$$\frac{\omega_E^2}{\omega_A^2} = \frac{C - B}{B} = \frac{-b_2^{'*}}{2\left(b_2^* + b_2^{'*}\right)}. \quad (60)$$

For a 246 potential the inverse susceptibilities have terms in q_4^4 and the squared values of the soft mode frequencies are not expected to scale linearly with q_4^2. The ratio of soft mode frequencies might be expected to follow

$$\frac{\omega_E^2}{\omega_A^2} = \frac{-b_2^{'*}q_4^2 - \frac{2}{3}c_2^{''}q_4^4}{2\left(b_2^* + b_2^{'*}\right)q_4^2 + 4\left(c_2 + c_2^{''}\right)q_4^4}. \quad (61)$$

Data from the literature for soft mode frequencies are summarized in Figure 8. They are not consistent with the predictions from the simplest view of 24 or 246 soft mode behavior. Hayward and Salje (1999) showed that the square of the E_g soft mode frequency in the tetragonal stability field scales linearly with q_4^2 calculated for their 246 potential. An analogous relationship, using octahedral rotations instead of a calculated order parameter, was found by Yamanaka et al. (2000). These observations apply to both soft modes since ω_E^2 scales linearly with ω_A^2 (ω_E^2/ω_A^2 = 0.117; Fig. 8b). Thus the expected result for a 24 potential, $\omega_E^2 \propto \omega_A^2 \propto q_4^2$, is obtained. On the other hand, the experimental ratio of the slopes for ω^2_F of the F_{2u} mode of the cubic phase to ω_A^2 of the tetragonal phase is ~1:2.6 as $T \rightarrow T_{c2}$. [Slopes were determined from the data of Shirane and Yamada (1969) over the temperature interval 112–140 K and from the data of Steigmeier and Auderset (1973) over the interval 91–103 K.] This ratio is intermediate between the ratios 1:2 and 1:4 for second order (24 potential) and tricritical (26 potential) transitions, respectively, as would be expected for structural evolution determined by a 246 potential.

A modified perspective on the soft mode behavior is that the frequencies scale with the susceptibilities of the unrenormalized Landau expansion (Slonczewski and Thomas 1970; Ishidate and Isonuma 1992). The second derivatives, $\partial^2 G/\partial q_i^2$, are taken from Equation 5 rather than Equation 12, with q_4 and the strains then set to their equilibrium values. This gives

$$\omega_A^2 \propto \chi_4^{-1} = \frac{\partial^2 G}{\partial q_4^2} = 2\left(b_2 + b_2'\right)q_4^2 + 4\left(c_2 + c_2''\right)q_4^4 \quad (62)$$

$$\omega_E^2 \propto \chi_6^{-1} = \frac{\partial^2 G}{\partial q_6^2} = \left(\frac{12\lambda_4^2}{\frac{1}{2}\left(C_{11}^o - C_{12}^o\right)} - b_2'\right)q_4^2 - \frac{2}{3}c_2''q_4^4. \quad (63)$$

The frequency of the soft mode in the cubic phase is expected to vary with temperature in the usual way as

$$\omega_F^2 \propto \chi^{-1} = \frac{\partial^2 G}{\partial q_i^2} = a\left(T + T_c\right). \quad (64)$$

Values for the ratios ω_E^2/ω_A^2 and ω_F^2/ω_A^2, calculated using Equations 62–64 and the preferred set of parameters listed in Table 6, can then be compared with the experimental values of 0.117 and 2.6. χ_4^{-1} and χ_6^{-1} vary linearly with temperature over a reasonable temperature range below T_c; straight lines fit to the calculated values between 90 and 105 K give a ratio of slopes of 0.138. The ratio of slopes for χ_4^{-1} and χ^{-1} is 2.9. These calculated variation of χ_4^{-1}, χ_6^{-1}, and χ^{-1} have been added to Figure 8a, with appropriate scaling, to show that ω^2 of the soft modes does not scale exactly with the susceptibilities. The square of the frequencies of the soft mode in tetragonal $SrTiO_3$ still scales more closely with q_4^2 (Fig. 8c).

Temperature dependence of C_{44}

The value of λ_5 extracted from the [111] stress dependence of the cubic → rhombohedral transition, 0.07 ± 0.02 GPa, has a relatively large uncertainty and is sensitive to the choice of value for λ_2. To constrain this parameter more tightly, C_{44} was calculated in the tetragonal stability field using the equation given in Table 2. A fit was found to the experimental data for C_{44} using trial values of λ_5 and c_2''. These values were used to recalculate b_2' (Eq. 14) and, hence, χ_6^{-1}. λ_5 and c_2'' were then adjusted again to obtain a new fit with C_{44}. The sequence of iterations was repeated, including iterations for b_2^* and $b_2'^*$ to fit $P_{111,t}$ at 4.2 K and 78. This sequence yielded $\lambda_5 = 0.125$ and $c_2'' = 0.00018$ GPa. Since $(c_2 + c_2'')$ = 0.001092 GPa from Hayward and Salje (1999), $c_2 = 0.000912$ GPa is obtained. Final values of $b_2 = 0.001152$ and $b_2' = 0.000076$ GPa were then obtained using Equations 13 and 14.

Elastic constant variations in tetragonal $SrTiO_3$

Data for C_{11}^o, C_{12}^o, C_{44}^o, and C_{44} have been used to extract values for the parameters in the Landau expansion and cannot, therefore, be used to test the validity of Equation 5 for describing the $Pm\bar{3}m \leftrightarrow I4/mcm$ transition. On the other hand, data for C_{11}, C_{33}, C_{12}, and C_{13} in the stability field of the $I4/mcm$ structure have not yet been used, and comparison of their experimental variations with variations determined from Equation 5 and the values of parameters listed in Table 6 provides an independent test of the model. First of all, however, the compilation of data from the literature reveals some inconsistencies in the experimental measurements. Ultrasonic data for C_{11} or C_{33} clearly show so much scatter that they cannot be regarded as being indicative of the intrinsic elastic properties of $SrTiO_3$ below 106 K. This is because any component of tetragonal stress applied at sufficiently low frequency will cause domain wall motions and an apparent softening which is much greater than the intrinsic softening due to the phase transition (Schranz et al. 1999; Kityk et al. 2000a, 2000b; Harrison et al. 2003). On the other hand, the Brillouin data reveal a much more self-consistent picture, as if they are more or less independent of domain wall or defect mobilities. They still do not define unique trends for C_{11} and C_{33}, but perhaps this is simply a matter of experimental uncertainties and the usual problem of correctly identifying propagation directions when dealing with intimately twinned crystals. Finally, the data of Lei and Ledbetter in Scott and Ledbetter (1997) for C_{44} seem more likely to have been measurements of C_{66}. The calculated variations of C_{11}, C_{33}, and C_{12} provide a semi-quantitative match with the observed variations from Brillouin scattering. In particular, the non-linear trends of softening as $T \rightarrow T_{c2}$ are reproduced. C_{44} is a fit to the data but reproduces the non-linear softening at $T \rightarrow T_{c2}$. Both these non-linear trends are due to the 246 character of the transition. A classically second order transition (24 potential) would give more or less constant values of C_{11}, C_{33}, C_{12}, C_{13}, and C_{44} with the same weak temperature dependence as C_{11}^o, C_{12}^o, and C_{44}^o.

Following Rehwald (1970b), Fossheim and Berre (1972), Slonczewski and Thomas (1970), and Hehlen et al. (1996), it has been assumed here that C_{66} is not affected by the $Pm\bar{3}m \leftrightarrow I4/mcm$ transition. The lowest order coupling term allowed by symmetry that would lead to a change in C_{66} would be of the form $\lambda e_6^2 q_4^2$. This would give $C_{66} = C_{44}^o + 2\lambda q_4^2$, and a predicted scaling of $(C_{66} - C_{44}^o)$ with q_4^2. The small difference between C_{66} and C_{44}^o could probably be fit using this expression but is only of similar magnitude to the uncertainty in the extrapolation of C_{44}^o.

Finally, the compilation of C_{44} data in Figure 3 highlights the substantial influence of the ferroelectric transition in ^{18}O enriched samples on the elastic constants below ~25 K (Itoh et al. 1999;

Yamaguchi et al. 2001; Yagi et al. 2002; Hasebe et al. 2002, 2003). To emphasize this, the split acoustic modes reported by these authors have simply been converted to elastic constants here without consideration of which elastic constants they refer to. Similar anomalies are not observed for C_{11} and C_{33}. In contrast, the compiled data for C_{44} of ^{16}O samples appear to show only a small deviation from the trend for the *I*4/*mcm* structure below ~37 K (Courtens et al. 1993; Hehlen et al. 1996, 1999; Balashova et al. 1996). Müller et al. (1991) and many subsequent authors have discussed evidence for a phase transition at this temperature. Again, there is little evidence for an anomaly in the combined data for C_{11} and C_{33}.

Bulk and shear moduli of polycrystalline perovskites are of more interest in a geophysical context than the single crystal moduli. For the cubic phase, these are usually given explicitly for the bulk modulus and by the average of Voigt and Reuss limits for the shear modulus as

$$K^o = \frac{1}{3}\left(C_{11}^o + 2C_{12}^o\right) \tag{65}$$

$$G^o = \frac{1}{2}\left(G_V + G_R\right) = \frac{1}{2}\left[\frac{1}{5}\left(C_{11}^o - C_{12}^o + 3C_{44}^o\right) + 5\left(\frac{4}{\left(C_{11}^o - C_{12}^o\right)} + \frac{3}{C_{44}^o}\right)^{-1}\right]. \tag{66}$$

Values for K^o and G^o have been calculated using the temperature dependent variations of the bare elastic constants given by Equation 39. For the tetragonal structure, K and G are the average of Voigt and Reuss limits, as given by expressions from Watt and Peselnik (1980)

$$K_V = \frac{1}{9}\left[2\left(C_{11} + C_{12}\right) + C_{33} + 4C_{13}\right] \tag{67}$$

$$G_V = \frac{1}{30}\left[C_{11} + C_{12} + 2C_{33} - 4C_{13} + 3\left(C_{11} - C_{12}\right) + 12C_{44} + 6C_{66}\right] \tag{68}$$

$$K_R = \frac{\left(C_{11} + C_{12}\right)C_{33} - 2C_{13}^2}{C_{11} + C_{12} + 2C_{33} - 4C_{13}} \tag{69}$$

$$G_R = 15\left[\frac{18K_V}{\left(\left(C_{11} + C_{12}\right)C_{33} - 2C_{13}^2\right)} + \frac{6}{\left(C_{11} - C_{12}\right)} + \frac{6}{C_{44}} + \frac{3}{C_{66}}\right]^{-1}. \tag{70}$$

Calculated bulk and shear moduli using the single-crystal elastic constants obtained here are shown in Figure 9. There appear to be no direct experimental determinations of the bulk and shear moduli as a function of temperature for polycrystalline $SrTiO_3$ for comparison with the calculated variations. The most distinctive features of their variations, however, are the discontinuities at the transition point. For the Voigt limits, the bulk and shear moduli in the *I*4/*mcm* stability field can be given, alternatively, by

$$K_V = \frac{1}{3}\left(C_{11}^o + 2C_{12}^o\right) - 4\lambda_2^2\chi_4 q_4^2 \tag{71}$$

$$G_V = \frac{1}{5}\left(C_{11}^o - C_{12}^o + 3C_{44}^o\right) - \frac{2}{5}\left(8\lambda_4^2\chi_4 + \lambda_5^2\chi_6\right)q_4^2. \tag{72}$$

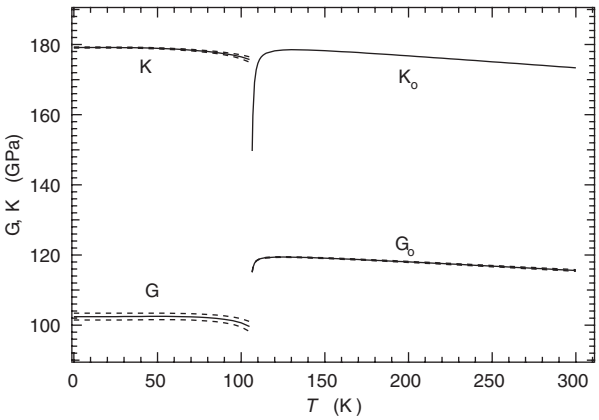

FIGURE 9. Calculated variations of the bulk (K) and shear (G) moduli of $SrTiO_3$. Softening as $T \rightarrow T_{c2}$ from above the transition point has been included, though calculated values are shown only down to T_{c2} + 1 K. Reuss and Voigt limits for the tetragonal structure are shown as broken lines; the solid lines represent the average of these two limiting cases. No attempt has been made to include the additional softening of C_{44} below ~40 K.

The important parameters in this context are the coupling coefficients λ_2, λ_4, and λ_5. The anomaly in K is small as a direct consequence of the fact that the coupling between octahedral tilting and volume strain is weak. The anomaly in G is large because the coupling between octahedral tilting and shear strain is much stronger. Softening as $T \rightarrow T_{c2}$ from above is based on Equation 40 and the fit parameters given earlier. Values are only given down to T_{c2} + 1 K in Figure 9 because they become progressively less reliable at small ΔT. The limit of possible softening near T_{c2} is not known.

DISCUSSION

Equation 5 leads to expressions for the variations of the elastic constants of $SrTiO_3$ that reproduce the main features of the $Pm\bar{3}m \leftrightarrow$ *I*4/*mcm* transition from the transition point down to ~0 K. The temperature dependence of C_{11}, C_{33}, C_{12}, C_{13}, and C_{44}, in particular, are consistent with a substantial contribution to the excess free energy from sixth order terms in the Landau expansion. This result is consistent with the view of Salje et al. (1998) and Hayward and Salje (1999) that the transition conforms closely to mean field behavior. On the other hand, a 246 Landau potential predicts subtle differences in phonon frequencies in comparison with those expected from a classical model of the soft mode. One possibility is that the macroscopic strain has a dominant influence on the soft mode frequency such that ω^2 scales with e_t rather than χ_4^{-1} or χ_6^{-1}. Another possibility is that the transition is in fact closer to second order in character than implied by the 246 potential, but that there is a break in the evolution of the order parameter some tens of K below T_{c2}, similar to that found for the cubic $\leftrightarrow$ rhombohedral transition in $LaAlO_3$ (Hayward et al. 2005).

Several choices have had to be made during the course of the parameterization, and the resulting set of coefficients represents a self-consistent solution rather than a unique solution. One obvious compromise has been the use of a single, temperature-

independent value of λ_2 to describe coupling between the order parameter and the volume strain. Non-linear variations of transition temperature with pressure (Fig. 4a) and volume strain with q_4^2 (Fig. 7c) imply that this assumption may not be correct. The non-linearity in Figure 4a could be explained by λ_2 having a temperature- or pressure-dependence, while the non-linearity in Figure 7b could imply coupling of the volume strain with higher order terms in q_4. It appears that coupling with the volume strain is very weak just below T_{c2}. If $\lambda_2 = 0$ is used in Equation 53 (but keeping $\lambda_4 = -0.075$ GPa), a slope of 93 K/GPa is obtained for the effect of a biaxial stress on the transition temperature. This is indistinguishable from the experimental value of 92 ± 3 K/GPa from Fossheim and Berre (1972). Similarly, assuming $\lambda_2 = 0$, but keeping $\lambda_5 = 0.125$ GPa, gives a slope of 41 K/GPa for the effect of a [111] stress on the pseudo-cubic ↔ rhombohedral transition temperature (Eq. 49). This is closer to the experimental value of ~35 ± 6 K/GPa from the data of Müller et al. (1970) than the value of 53 K/GPa obtained when $\lambda_2 = 0.046$ is used. The volume strain might or might not be very small in an interval of up to ~20 K below T_c, but it certainly increases in magnitude below ~80 K. If there is a similar increase in the strength of coupling with increasing pressure, the values calculated for q_5^2 with increasing [111] stress would also increase. The difference between observed and calculated variations of the order parameter in the $R\bar{3}c$ stability field (Fig. 6) would thus be reduced. High-resolution data for the lattice parameters of both cubic and tetragonal $SrTiO_3$ are needed to test these possibilities. A temperature- and/or pressure-dependence for λ_2, or higher order coupling between e_a and q_4, would have implications for the equilibrium evolution of the order parameter.

The present analysis differs from previous attempts to describe the elastic anomalies in $SrTiO_3$ using Landau theory in that all the symmetry-allowed sixth order terms and the influence of order parameter saturation have been included. The present model has also been tested against data collected over the entire stability field of the tetragonal structure rather than simply matching the step in elastic constants at the transition point. For the first time in the case of phase transitions in perovskites, a complete set of values for the coefficients in a 246 potential has been obtained, and these provide some insight into the driving energies. Slonczewski and Thomas (1970) pointed out that coupling of the order parameter with strain contributes to the stability of the *I*4/*mcm* structure relative to the $R\bar{3}c$ structure of $SrTiO_3$. The strength of coupling with e_t is in fact sufficient to change the value of $b_2'^*$ from positive to negative. If the coupling was weaker (smaller $|\lambda_4|$) $b_2'^*$ would be positive and the rhombohedral structure would be more stable than the tetragonal structure below T_{c2}. Individual contributions to the excess free energy, due to the order parameter coupling alone, $G(q)$, strain/order parameter coupling, $G(q,e)$, and Hooke's law elastic energy, G(elastic), can now also be calculated. At 50 K, for example, the total excess free energy due to the cubic → tetragonal transition is –4.63 J/mol and this is made up of $G(q) = -3.44$, $G(q,e) = -2.37$, G(elastic) = 1.18 J/mol. The main driving energy for the transition is due to the order parameter alone, but a significant contribution also comes from the coupling of the soft mode with strain.

The silicate perovskites $(Mg,Fe)SiO_3$ and $CaSiO_3$ can, in principle, undergo octahedral tilting transitions that are analogous to the transitions in $(Ca,Sr)TiO_3$ perovskites. The Landau expansions presented here, together with the methodology for determining values for all the relevant parameters, provide a basis for addressing the question of how such transitions might potentially influence the bulk elastic properties of the earth's mantle. The effects of hydrostatic pressure, non-hydrostatic stress and variable composition can be included as necessary. Any anomaly in bulk modulus accompanying cubic ↔ tetragonal or tetragonal ↔ orthorhombic transitions depends on the coupling with volume strain. The magnitude of this strain is likely to be small but, more significantly, it may be temperature (and/or pressure) dependent. A temperature dependence which was sufficient to change the sign of the coupling from positive to negative would reverse the sign of the pressure dependence of the transition temperature. Extrapolation of this slope from laboratory conditions to mantle pressures and temperatures is therefore highly uncertain. Cubic ↔ tetragonal and tetragonal ↔ orthorhombic transitions in silicate perovskites are likely to have a substantial effect on the shear modulus. A change of ~20%, as shown in Figure 9, would not be surprising. Quantitative analysis of the effects of the *I*4/*mcm* ↔ *Pnma* transition will require similar calibration of parameters for the M point instability.

Acknowledgements

This work was funded by a grant from the Natural Environment Research Council (NER/A/S/2000/01055), which is gratefully acknowledged.

References cited

Ang, C., Scott, J.F., Yu, Z., Ledbetter, H., and Baptista, J.L. (1999) Dielectric and ultrasonic anomalies at 16, 37, and 65 K in $SrTiO_3$. Physical Review B, 59, 6661–6664.

Axe, J.D. and Shirane, G. (1970) Study of the α-β quartz phase transformation by inelastic neutron scattering. Physical Review B, 1, 342–348.

Balashova, E.V., Lemanov, V.V., Kunze, R., Martin, G., and Weihnacht, M. (1996) Ultrasonic study on the tetragonal and Müller phase in $SrTiO_3$. Ferroelectrics, 183, 75–83.

Ball, C.J., Begg, B.D., Cookson, D.J., Thorogood, G.J., and Vance, E.R. (1998) Structures in the system $CaTiO_3/SrTiO_3$. Journal of Solid State Chemistry, 139, 238–247.

Bell, R.O. and Rupprecht, G. (1963) Elastic constants of strontium titanate. Physical Review, 129, 90–94.

Bianchi, U., Kleemann, W., and Bednorz, J.G. (1994) Raman scattering of ferroelectric $Sr_{1-x}Ca_xTiO_3$, x = 0.007. Journal of Physics: Condensed Matter, 6, 1229–1238.

Binder, A. and Knorr, K. (2001) Shear elasticity and ferroelastic hysteresis of the low-temperature phase of $SrTiO_3$. Physical Review B, 63, 094106.

Birgeneau, R.J., Kjems, J.K., Shirane, G., and Van Uitert, L.G. (1974) Cooperative Jahn-Teller phase transition in $PrAlO_3$. Physical Review B, 10, 2512–2534.

Bulou, A., Rousseau, M., and Nouet, J. (1992) Ferroelastic phase transitions and related phenomena. Key Engineering Materials, 68, 133–186.

Burke, W.J. and Pressley, R.J. (1969) Anomalous stress effects on the fluorescence of $SrTiO_3:Cr^{3+}$. Solid State Communications, 7, 1187–1190.

Burke, W.J., Pressley, R.J., and Slonczewski, J.C. (1971) Raman scattering and phase transitions in stressed $SrTiO_3$. Solid State Communications, 9, 121–124.

Caracas, R., Wentzcovitch, R., Price, G.D., and Brodholt, J. (2005) $CaSiO_3$ perovskite at lower mantle pressures. Geophysical Research Letters, 32, L06306 (DOI: 10.1029/2004GL022144).

Carpenter, M.A. (2007) Elastic anomalies accompanying phase transitions in $(Ca,Sr)TiO_3$ perovskites: Part II. Calibration for the effects of composition and pressure. American Mineralogist, 92, 328–343.

Carpenter, M.A. and Salje, E.K.H. (1998) Elastic anomalies in minerals due to structural phase transitions. European Journal of Mineralogy, 10, 693–812.

Carpenter, M.A., Becerro, A.I., and Seifert, F. (2001) Strain analysis of phase transitions in $(Ca,Sr)TiO_3$ perovskites. American Mineralogist, 86, 348–363.

Carpenter, M.A., Meyer, H.-W., Sondergeld, P., Marion, S., and Knight, K.S. (2003) Spontaneous strain variations through the low temperature phase transitions of deuterated lawsonite. American Mineralogist, 88, 534–546.

Carpenter, M.A., Li, B., and Liebermann, R.C. (2007) Elastic anomalies accompanying phase transitions in $(Ca,Sr)TiO_3$ perovskites: Part III. Experimental inves-

tigation of polycrystalline samples. American Mineralogist, 92, 344–355.
Courtens, E., Coddens, G., Hennion, B., Hehlen, B., Pelous, J., and Vacher, R. (1993) Phonon anomalies in $SrTiO_3$ in the quantum paraelectric regime. Physica Scripta, T49, 430–435.
Cowley, R.A. (1996) The phase transition in strontium titanate. Philosophical Transactions of the Royal Society of London A, 354, 2799–2814.
Cowley, R.A., Buyers, W.J.L., and Dolling, G. (1969) Relationship of normal modes of vibration of strontium titanate and its antiferroelectric phase transition at 110 K. Solid State Communications, 7, 181–184.
Cummins, H.Z. (1979) Brillouin scattering spectroscopy of ferroelectric and ferroelastic phase transitions. Philosophical Transactions of the Royal Society of London A, 293, 393–405.
Darlington, C.N.W. (1997) Landau theory applied to transitions in $BaCeO_3$ and $PrAlO_3$. Physica Status Solidi (b), 203, 73–78.
Devonshire, A.F. (1949) Theory of barium titanate, Part I. Philosophical Magazine, 40, 1040–1067.
——— (1951) Theory of barium titanate, Part II. Philosophical Magazine, 42, 1065–1079.
Fiquet, G., Andrault, D., Dewaele, A., Charpin, T., Kunz, M., and Haüsermann, D. (1998) *P-V-T* equation of state of $MgSiO_3$ perovskite. Physics of the Earth and Planetary Interiors, 105, 21–31.
Fleury, P.A., Scott, J.F., and Worlock, J.M. (1968) Soft phonon modes and the 110 K phase transition in $SrTiO_3$. Physical Review Letters, 21, 16–19.
Fossheim, K. and Berre, B. (1972) Ultrasonic propagation, stress effects, and interaction parameters at the displacive transition in $SrTiO_3$. Physical Review B, 5, 3292–3308.
Fossum, J.O. (1985) A phenomenological analysis of ultrasound near phase transitions. Journal of Physics C, 18, 5531–5548.
Grzechnik, A., Wolf, G.H., and McMillan, P.F. (1997) Raman scattering study of $SrTiO_3$ at high pressure. Journal of Raman Spectroscopy, 28, 885–889.
Guyot, F., Richet, P., Courtial, Ph., and Gillet, Ph. (1993) High-temperature heat capacity and phase transitions of $CaTiO_3$ perovskite. Physics and Chemistry of Minerals, 20, 141–146.
Harley, R.T., Hayes, W., Perry, A.M., and Smith, S.R.P. (1973) The phase transitions of $PrAlO_3$. Journal of Physics C, 6, 2382–2400.
Harrison, R.J., Redfern, S.A.T., and Street, J. (2003) The effect of transformation twins on the seismic-frequency mechanical properties of polycrystalline $Ca_{1-x}Sr_xTiO_3$ perovskite. American Mineralogist, 88, 574–582.
Hasebe, H., Tsujimi, Y., Wang, R., Itoh, M., and Yagi, T. (2002) Brillouin scattering study of ferroelectric $SrTi(^{18}O_x{}^{16}O_{1-x})_3$. Ferroelectrics, 272, 39–44.
——— (2003) Dynamical mechanism of the ferroelectric phase transition of $SrTi^{18}O_3$ studied by light scattering. Physical Review B, 68, 014109.
Hayward, S.A. and Salje, E.K.H. (1999) Cubic-tetragonal phase transition in $SrTiO_3$ revisited: Landau theory and transition mechanism. Phase Transitions, 68, 501–522.
Hayward, S.A., Morrison, F.D., Redfern, S.A.T., Salje, E.K.H., Scott, J.F., Knight, K.S., Tarantino, S., Glazer, A.M., Shuvaeva, V., Daniel, P., Zhang, M., and Carpenter, M.A. (2005) Transformation processes in $LaAlO_3$: neutron diffraction, dielectric, thermal, optical, and Raman studies. Physical Review B, 72, 054110.
Hehlen, B., Kallassy, Z., and Courtens, E. (1996) The high-frequency elastic constants of $SrTiO_3$ in the quantum paraelectric regime. Ferroelectrics, 183, 265–272.
Hehlen, B., Arzel, L., Tagantsev, A.K., Courtens, E., Inaba, Y., Yamanaka, A., and Inoue, K. (1999) Observation of the coupling between TA and TO modes in $SrTiO_3$ by Brillouin scattering. Physica B, 263–264, 627–631.
Höchli, U.T. (1972) Elastic constants and soft optical modes in gadolinium molybdate. Physical Review B, 6, 1814–1823.
Howard, C.J. and Stokes, H.T. (1998) Group-theoretical analysis of octahedral tilting in perovskites. Acta Crystallographica B, 54, 782–789.
Ishidate, T. and Isonuma, T. (1992) Phase transition of $SrTiO_3$ under high pressure. Ferroelectrics, 137, 45–52.
Ishidate, T., Sasaki, S., and Inoue, K. (1988) Brillouin scattering of $SrTiO_3$ under high pressure. High Pressure Research, 1, 53–65.
Itoh, M., Wang, R., Inaguma, Y., Yamaguchi, T., Shan, Y.-J., and Nakamura, T. (1999) Ferroelectricity induced by oxygen isotope exchange in strontium titanate perovskite. Physical Review Letters, 82, 3540–3543.
Jung, D.Y. and Oganov, A.R. (2005) Ab initio study of the high-pressure behavior of $CaSiO_3$ perovskite. Physics and Chemistry of Minerals, 32, 146–153.
Kennedy, B.J., Howard, C.J., and Chakoumakos, B.C. (1999) Phase transitions in perovskite at elevated temperatures—a powder neutron diffraction study. Journal of Physics: Condensed Matter, 11, 1479–1488.
Kityk, A.V., Schranz, W., Sondergeld, P., Havlik, D., Salje, E.K.H., and Scott, J.F. (2000a) Low-frequency superelasticity and nonlinear elastic behavior of $SrTiO_3$ crystals. Physical Review B, 61, 946–956.
——— (2000b) Nonlinear elastic behavior of $SrTiO_3$ crystals in the quantum paraelectric regime. Europhysics Letters, 50, 41–47.
Kurashina, T., Hirose, K., Ono, S., Sata, N., and Ohishi, Y. (2004) Phase transition in Al-bearing $CaSiO_3$ perovskite: implications for seismic discontinuities in the lower mantle. Physics of the Earth and Planetary Interiors, 145, 67–74.
Laubereau, A. and Zurek, R. (1970) Brillouin-Streuung in Strontiumtitanat-Einkristallen im Temperaturbereich 5 K bis 300 K. Zeitschrift für Naturforschung, 25a, 391–401.
Lemanov, V.V., Gridnev, S.A., and Ukhin, E.V. (2002) Low-frequency elastic properties, domain dynamics, and spontaneous twisting of $SrTiO_3$ near the ferroelastic phase transition. Physics of the Solid State, 44, 1156–1165.
Liu, M., Finlayson, T.R., and Smith, T.F. (1997) High-resolution dilatometry measurements of $SrTiO_3$ along cubic and tetragonal axes. Physical Review B, 55, 3480–3484.
Lüthi, B. and Moran, T.J. (1970) Sound propagation near the structural phase transition in strontium titanate. Physical Review B, 2, 1211–1214.
Lüthi, B. and Rehwald, W. (1981) Ultrasonic studies near structural phase transitions. In K.A. Müller and H. Thomas, Eds., Structural phase transitions I, Topics in Current Physics, 23, p. 131–184. Springer-Verlag, Berlin.
Meyer, H.-W., Carpenter, M.A., Graeme-Barber, A., Sondergeld, P., and Schranz, W. (2000) Local and macroscopic order parameter variations associated with low temperature phase transitions in lawsonite, $CaAl_2Si_2O_7(OH)_2{\cdot}H_2O$. European Journal of Mineralogy, 12, 1139–1150.
Meyer, H.-W., Marion, S., Sondergeld, P., Carpenter, M.A., Knight, K.S., Redfern, S.A.T., and Dove, M.T. (2001) Displacive components of the low-temperature phase transitions in lawsonite. American Mineralogist, 86, 566–577.
Migliori, A., Sarrao, J.L., Visscher, W.M., Bell, T.M., Lei, M., Fisk, Z., and Leisure, R.G. (1993) Resonant ultrasound spectroscopic techniques for measurement of the elastic moduli of solids. Physica B, 183, 1–24.
Mishra, S.K., Ranjan, R., Pandey, D., Ranson, P., Ouillon, R., Pinan-Lucarre, J.-P., and Pruzan, P. (2005) A combined X-ray diffraction and Raman scattering study of the phase transitions in $Sr_{1-x}Ca_xTiO_3$ (x = 0.04, 0.06, 0.12). Journal of Solid State Chemistry, 178, 2846–2857.
Mishra, S.K., Ranjan, R., Pandey, D., and Stokes, H.T. (2006a) Resolving the controversies about the 'nearly cubic' and other phases of $Sr_{1-x}Ca_xTiO_3$ ($0 \le x \le 1$): I. Room temperature structures. Journal of Physics: Condensed Matter, 18, 1885–1898.
Mishra, S.K., Ranjan, R., Pandey, D., Ranson, P., Ouillon, R., Pinan-Lucarre, J.-P., and Pruzan, P. (2006b) Resolving the controversies about the 'nearly cubic' and other phases of $Sr_{1-x}Ca_xTiO_3$ ($0 \le x \le 1$): II. Comparison of phase transition behaviours for x = 0.40 and 0.43. Journal of Physics: Condensed Matter, 18, 1899–1912.
Mitsui, T. and Westphal, W.B. (1961) Dielectric and X-ray studies of $Ca_xBa_{1-x}TiO_3$ and $Ca_xSr_{1-x}TiO_3$. Physical Review, 124, 1354–1359.
Müller, K.A., Berlinger, W., and Slonczewski, J.C. (1970) Order parameter and phase transitions of stressed $SrTiO_3$. Physical Review Letters, 25, 734–737.
Müller, K.A., Berlinger, W., and Tosatti, E. (1991) Indication for a novel phase in the quantum paraelectric regime of $SrTiO_3$. Zeitshcrift für Physik B, 84, 277–283.
Nye, J.F. (1985) Physical properties of crystals, 329 p. Oxford University Press, U.K.
Okai, B. and Yoshimoto, J. (1975) Pressure dependence of the structural phase transition temperature in $SrTiO_3$ and $KMnF_3$. Journal of the Physical Society of Japan, 39, 162–165.
Okazaki, A. and Kawaminami, M. (1973) Lattice constant of strontium titanate at low temperatures. Materials Research Bulletin, 8, 545–550.
Ono, S., Kikegawa, T., and Iizuka, T. (2004a) The equation of state of orthorhombic perovskite in a peridotitic mantle composition to 80 GPa: implications for chemical composition of the lower mantle. Physics of the Earth and Planetary Interiors, 145, 9–17.
Ono, S., Ohishi, Y., and Mibe, K. (2004b) Phase transition of Ca-perovskite and stability of Al-bearing Mg-perovskite in the lower mantle. American Mineralogist, 89, 1480–1485.
Pietrass, B. and Hegenbarth, E. (1969) Stress dependence of the phase transition near 100 K in $SrTiO_3$. Physica Status Solidi, 34, K119–K121.
Pytte, E. (1970) Soft-mode damping and ultrasonic attenuation at a structural phase transition. Physical Review B, 1, 924–930.
——— (1971) Acoustic anomalies at structural phase transitions. In E.J. Samulsen, E. Anderson, and J. Feder, Eds., Structural phase transitions and soft modes, p. 151–169. NATO ASI, Norway, Scandinavian University Books, Oslo.
Qin, S., Becerro, A.I., Seifert, F., Gottsmann, J., and Jiang, J. (2000) Phase transitions in $Ca_{1-x}Sr_xTiO_3$ perovskites: effects of composition and temperature. Journal of Materials Chemistry, 10, 1609–1615.
Qin, S., Wu, X., Seifert, F., and Becerro, A.I. (2002) Micro-Raman study of perovskites in the $CaTiO_3$-$SrTiO_3$ system. Journal of the Chemical Society, Dalton Transactions, 2002, 3751–3755.
Ranjan, R. and Pandey, D. (2001a) Antiferroelectric phase transition in $(Sr_{1-x}Ca_x)TiO_3$ ($0.12 < x \le 0.40$): I. Dielectric studies. Journal of Physics: Condensed Matter, 13, 4239–4249.
——— (2001b) Antiferroelectric phase transition in $(Sr_{1-x}Ca_x)TiO_3$: II. X-ray diffraction studies. Journal of Physics: Condensed Matter, 13, 4251–4266.
Ranjan, R., Pandey, D., Schuddinck, W., Richard, O., De Meulenaere, P., Van Landuyt, J., and Van Tendeloo, G. (2001) Evolution of crystallographic phases

in $(Sr_{1-x}Ca_x)TiO_3$ with composition (x). Journal of Solid State Chemistry, 162, 20–28.
Ranson, P., Ouillon, R., Pinan-Lucarre, J.-P., Pruzan, P., Mishra, S.K., Ranjan, R., and Pandey, D. (2005) The various phases of the system $Sr_{1-x}Ca_xTiO_3$—a Raman scattering study. Journal of Raman Spectroscopy, 36, 898–911.
Redfern, S.A.T. (1996) High-temperature structural phase transitions in perovskite ($CaTiO_3$). Journal of Physics: Condensed Matter, 8, 8267–8275.
Rehwald. W. (1970a) Anomalous ultrasonic attenuation at the 105 K transition in strontium titanate. Solid State Communications, 8, 607–611.
——— (1970b) Low temperature elastic moduli of strontium titanate. Solid State Communications, 8, 1483–1485.
——— (1971) Ultrasonic properties of strontium titanate at the 105 K transition. Physik der Kondensierten Materie, 14, 21–36.
——— (1973) The study of structural phase transitions by means of ultrasonic experiments. Advances in Physics, 22, 721–755.
——— (1977) Critical behavior of strontium titanate under stress. Solid State Communications, 21, 667–670.
Salje, E.K.H., Wruck, B., and Thomas, H. (1991a) Order-parameter saturation and low-temperature extension of Landau theory. Zeitschrift für Physik B: Condensed Matter, 82, 399–404.
Salje, E.K.H., Wruck, B., and Marais, S. (1991b) Order parameter saturation at low temperatures—numerical results for displacive and o/d systems. Ferroelectrics, 124, 185–188.
Salje, E.K.H., Gallardo, M.C., Jiménez, J., Romero, F.J., and del Cerro, J. (1998) The cubic-tetragonal phase transition in strontium titanate: excess specific heat measurements and evidence for a near-tricritical, mean field type transition mechanism. Journal of Physics: Condensed Matter, 10, 5535–5543.
Sato, M., Soejima, Y., Ohama, N., Okazaki, A., Scheel, H.J., and Müller, K.A. (1985) The lattice constant vs. temperature relation around the 105 K transition of a flux-grown $SrTiO_3$ crystal. Phase Transitions, 5, 207–218.
Schranz, W., Sondergeld, P., Kityk, A.V., and Salje, E.K.H. (1999) Elastic properties of $SrTiO_3$ crystals at ultralow frequencies. Phase Transitions, 69, 61–76.
Scott, J.F. (1999) Comment on the physical mechanisms of the 37 and 65 K anomalies in strontium titanate. Journal of Physics: Condensed Matter, 11, 8149–8153.
Scott, J.F. and Ledbetter, H. (1997) Interpretation of elastic anomalies in $SrTiO_3$ at 37 K. Zeitschrift für Physik B, 104, 635–639.
Shirane, G. and Yamada, Y. (1969) Lattice-dynamical study of the 110 K phase transition in $SrTiO_3$. Physical Review, 177, 858–863.
Slonczewski, J.C. (1970) Analysis of stress and temperature dependence of fluorescence in $SrTiO_3:Cr^{3+}$. Physical Review B, 2, 4646–4655.
Slonczewski, J.C. and Thomas, H. (1970) Interaction of elastic strain with the structural transition of strontium titanate. Physical Review B, 1, 3599–3608.
Sondergeld, P., Schranz, W., Kityk, A.V., Carpenter, M.A., and Libowitzky, E. (2000) Ordering behavior of the mineral lawsonite. Phase Transitions, 71, 189–203.
Sorge, G., Hegenbarth, E., and Schmidt, G. (1970) Mechanical relaxation and nonlinearity in strontium titanate single crystals. Physica Status Solidi, 37, 599–603.
Steigmeier, E.F. and Auderset, H. (1973) Dynamic critical behavior at the structural phase transition in $SrTiO_3$. Solid State Communications, 12, 565–568.
Stixrude, L. and Cohen, R.E. (1993) Stability of orthorhombic $MgSiO_3$ perovskite in the earth's lower mantle. Nature, 364, 613–615.
Stokes, H.T. and Hatch, D.M. (1988) Isotropy subgroups of the 230 crystallographic space groups. World Scientific, Singapore.
Stokowski, S.E. and Schawlow, A.L. (1969) Spectroscopic studies of $SrTiO_3$ using impurity-ion probes. Physical Review, 178, 457–464.
Thomas, H. and Müller, K.A. (1968) Structural phase transitions in perovskite-type crystals. Physical Review Letters, 21, 1256–1259.
Vanderbilt, D. and Cohen, M.H. (2001) Monoclinic and triclinic phases in higher-order Devonshire theory. Physical Review B, 63, 094108.
Watt, J.P. (1979) Hashin-Shtrikman bounds on the effective elastic moduli of polycrystals with orthorhombic symmetry. Journal of Applied Physics, 50, 6290–6295.
Watt, J.P. and Peselnik. L. (1980) Clarification of the Hashin-Shtrikman bounds on the effective elastic moduli of polycrystals with hexagonal, trigonal, and tetragonal symmetries. Journal of Applied Physics, 51, 1525–1531.
Wentzcovitch, R.M., Martins, J.L., and Price, G.D. (1993) Ab initio molecular dynamics with variable cell shape: application to $MgSiO_3$. Physical Review Letters, 70, 3947–3950.
Yagi, T., Kasahara, M., Tsujimi, Y., Yamaguchi, M., Hasebe, H., Wang, R., and Itoh, M. (2002) Brillouin and Raman scattering study of the isotopically induced ferroelectric phase transition of $SrTi^{18}O_3$. Physica B, 316–317, 596–599.
Yamaguchi, M., Yagi, T., Wang, R., and Itoh, M. (2001) Light scattering study of the ferroelectric phase transition in $SrTi^{18}O_3$. Physical Review B, 63, 172102.
Yamaguchi, M., Yagi, T., Tsujimi, Y., Hasebe, H., Wang, R., and Itoh, M. (2002) Brillouin-scattering study of the broad doublet in isotopically exchanged $SrTiO_3$. Physical Review B, 65, 172102.
Yamanaka, A., Kataoka, M., Inaba, Y., Inoue, K., Hehlen, B., and Courtens, E. (2000) Evidence for competing orderings in strontium titanate from hyper-Raman scattering spectroscopy. Europhysics Letters, 50, 688–694.
Yamanaka, T., Hirai, N., and Komatsu, Y. (2002) Structure change of $Ca_{1-x}Sr_xTiO_3$ perovskite with composition and pressure. American Mineralogist, 87, 1183–1189.
Yao, W., Cummins, H.Z., and Bruce, R.H. (1981) Acoustic anomalies in terbium molybdate near the improper ferroelastic-ferroelectric phase transition. Physical Review B, 24, 424–444.

MANUSCRIPT RECEIVED APRIL 27, 2006
MANUSCRIPT ACCEPTED SEPTEMBER 28, 2006
MANUSCRIPT HANDLED BY GEORGE LAGER